

بسم الله الرحمن الرحيم



Sudan University of Science & Technology  
Faculty of Graduate Studies



*Gamma Rays Induced Effects on the Performance of  
Silicon Solar Cells*

تأثير أشعة غاما المستحثة على جودة أداء الخلايا الشمسية السيليكونية

*Thesis Submitted In Fulfillment for The Requirements of P.hD In Physics*

**By:**

*Afraa Khamies Kajo Konda*

**Supervisor:**

*Dr. Ahmed Alhassan Alfaki Idris*

**Co Supervisor:**

*Dr. Nassreldeen Abdelrazig Abdelbari Elsheikh*

*December, 2019*

قَالَ تَعَالَى:

﴿ وَقُلْ أَعْمَلُوا فَسَيَرَى اللَّهُ عَمَلَكُمْ وَرَسُولُهُ وَالْمُؤْمِنُونَ وَسَتُرَدُّونَ إِلَىٰ

عِلْمِ الْغَيْبِ وَالشَّهَادَةِ فِيمَا كُنْتُمْ تَعْمَلُونَ ﴿١٠٥﴾

صدق الله العظيم

التوبة: ١٠٥

# DEDICATION

*To my great father and my dear mother.*

*To those who give more than take.. my friends.*

*To all my teachers.*

*And to those whom I love.*

## ACKNOWLEDGEMENTS

*Thanks for god for his guidance in all my academic years. My thanks and gratitude to my supervisor Dr. Ahmed Alhassan Alfaki Idris . Special thanks to my Co- supervisor and mentor Dr .Nassreldeen Abdelrazig Abdelbari Elsheikh, and lots of thanks to Sudan Atomic Energy Commission, and special thanks for all the people who supported me through the way out .....*

# ABSTRACT

This work explores the effects of  $^{60}\text{Co}$  and  $^{137}\text{Cs}$   $\gamma$ -irradiation on the Photovoltaic parameters of mono-crystalline silicon solar cells. Two suitable (light source- solar cell) geometry were instrumented. They consist of a halogen lamp of 500W power and  $100\text{mW}\cdot\text{cm}^{-2}$  light intensity, and a mono-crystalline silicon solar cell with an active area of  $10\text{cm}\times 5\text{cm}$  for each geometry. At room temperature, the forward bias (I-V) and (P-V) characteristics were determined under illumination, before and after irradiation with different  $^{60}\text{Co}$   $\gamma$ -exposure doses; 532 mR, 1064 mR and 1596mR, for the first solar cell and different  $^{137}\text{Cs}$   $\gamma$ -exposure doses; 280 mR, 560 mR and 837mR for the second cell for 1hr,2hrs, 3hrs , respectively. The results demonstrated that  $\gamma$ -exposure doses have a significant effect on the photovoltaic parameters and it controls the quality and performance of the solar cell. The open circuit voltage ( $V_{oc}$ ), short circuit current ( $I_{sc}$ ), maximum output power ( $P_m$ ), fill factor (FF) and efficiency ( $\eta$ ) are found to be decreased with different gamma exposure doses.

For  $^{60}\text{Co}$   $\gamma$ -exposure the  $V_m$  values were decreased by 0.4%, 2.9% and 9%, respectively while  $I_m$  values were deteriorated by 9.7%, 12% and 17.5%, respectively. Consequently, the  $P_m$  values were deteriorated by approximately by 10%, 14.5% and 24.9%, respectively. The  $V_{oc}$  and  $I_{sc}$  values were deteriorated by

approximately by 1.5%, 2.2% and 3% for  $V_{oc}$ , and 3%, 6% and 11.9% for  $I_{sc}$ , respectively.

On the other hand, the FF values were deteriorated by approximately 5.9%, 7.1% and 12.2%, while the  $\eta$  values deteriorated by 9%, 13.4% and 24% respectively.

Similarly For  $^{137}\text{Cs}$   $\gamma$ -exposure the  $V_m$  values were decreased by 0.4%, 2.9% and 9%, respectively while  $I_m$  values were deteriorated by 7.9%, 10.1% and 13.3%, respectively.

Consequently, the  $P_m$  values were deteriorated by approximately 8.3%, 12.8% and 21%, respectively. The  $V_{oc}$  and  $I_{sc}$  values were deteriorated by approximately 0.9%, 1.6% and 2% for  $V_{oc}$ , and 2%, 5% and 10.9 % for  $I_{sc}$ , respectively. On the other hand, the FF values were deteriorated by approximately 5.5%, 6.8% and 9.7%, while the  $\eta$  values deteriorated by 7.1 %, 11.7% and 20.2% respectively.

When the reduction of the I-V characteristics caused by  $^{60}\text{Co}$   $\gamma$ -ray photons were compared with those caused by  $^{137}\text{Cs}$   $\gamma$ -ray photons at the same acquisition time (1,2,3 hours) , it was found that the  $V_{mp}$  reduction caused by  $^{60}\text{Co}$   $\gamma$ -ray photons exceeds that of  $^{137}\text{Cs}$   $\gamma$ -ray photons by 0.04% , 0.0001 % , 0.001% respectively .while the  $I_{mp}$  reduction caused by  $^{60}\text{Co}$   $\gamma$ -ray photons exceeds that of  $^{137}\text{Cs}$   $\gamma$ -ray photons by 1.96% , 2 % , 4.9 % respectively .

On the other hand when comparing the P-V reduction caused by  $^{60}\text{Co}$   $\gamma$ -ray photons with that caused by  $^{137}\text{Cs}$   $\gamma$ -ray photons at the same acquisition time (1,2,3

hours) for both sources, it was found that the  $P_{mp}$  reduction caused by  $^{60}\text{Co}$   $\gamma$ -ray photons exceeds that of  $^{137}\text{Cs}$   $\gamma$ -ray photons by 2% 1.9% and 4.7% respectively. This may attribute to the fact that the average energy of  $^{60}\text{Co}$  (1.25 MeV) is higher than the energy of  $^{137}\text{Cs}$  (0.662 Mev).

The results re-confirmed the deterioration effect of induced  $^{60}\text{Co}$  and  $^{137}\text{Cs}$   $\gamma$  displacement damage on the photovoltaic parameters of mc-Si solar cell

## المستخلص

في هذه الأطروحة تم استخدام مصدرين مشعّين (كوبالت 60 و سيزيوم 137) لدراسة تأثير أشعة غاما على أداء وكفاءة خليتين شمسيّتين أحاديّتي البلورة . تم تشعيع الخلية الشمسية الأولى بجرعات مختلفة من الكوبالت-60, 532mR , 1064mR و 1596mR , وتشعيع الخلية الثانية بجرعات مختلفة من السيزيوم-137, 280mR , 560 mR و 837mR لمدة ساعة , ساعتان وثلاث ساعات على التوالي . وتم تحديد خصائص الانحياز الامامي , P-V I-V للخليتين عند درجة حرارة الغرفة قبل وبعد التشعيع .

أظهرت النتائج أن لأشعة غاما تأثير كبير على الخصائص الكهربية للخلية الشمسية وأنها تتحكم في جودة وأداء الخلية الشمسية بعد تشعيع الخلية الأولى وجد أن هناك إنخفاض حدث في قيم  $V_m$  بنسبة % 0.4 , % 2.9 و % 9 بعد التشعيع لمدة 3,2,1 ساعات على التوالي وكذلك إنخفضت قيمة  $I_m$  بنسبة % 9.7 , % 12 و % 17.5 على التوالي , وقيم ال  $P_m$  بنسبة % 10 , % 14.5 و % 24.9 كما إنخفضت قيم  $I_{sc}$   $V_{oc}$  بنسب مختلفة % 1.5 , % 2.2 و % 3 لل  $V_{oc}$  و % 3 و % 6 و % 11.9 لل  $I_{sc}$  . بالإضافة الي ذلك أظهرت النتائج إنخفاض ملحوظ في قيم ال Fill Factor و الكفاءة , فقد إنخفضت قيم ال FF بنسبة % 5.9 , % 7.1 و % 12.2 للجرعات الثلاث على التوالي , بينما إنخفضت قيم الكفاءة بنسبة % 9 , % 13.4 و % 24 بعد التشعيع بمصدر الكوبالت .

كذلك بينت النتائج بعد تشعيع الخلية الشمسية الثانية بأشعة غاما من مصدر السيزيوم 137 إنخفاض في قيم  $V_m$  بنسبة % 0.4 , % 2.9 و % 9 بعد التشعيع لمدة 3,2,1 ساعات على التوالي وكذلك إنخفضت في قيم  $I_m$  بنسبة % 7.9 , % 10.1 و % 13.4 على التوالي , وقيم ال  $P_m$  بنسبة % 8.3 , % 12.8 و % 21.1 . كما إنخفضت قيم  $I_{sc}$   $V_{oc}$  بنسب مختلفة , % 0.9 , % 1.6 و % 2 لل  $V_{oc}$  و % 2 , % 5 و % 10.9 لل  $I_{sc}$  . بالإضافة الي ذلك أظهرت النتائج إنخفاض ملحوظ في قيم ال Fill Factor و الكفاءة , فقد إنخفضت قيم ال FF بنسبة % 5.5 , % 6.8 و % 9.7 للجرعات الثلاث على التوالي , بينما إنخفضت قيم الكفاءة بنسبة % 1.7 , % 11.7 و % 20.2 بعد التشعيع .

وعندما قورنت نتائج الانخفاض في قيم الجهد والتيار والطاقة للخلية الشمسية الأولى بعد التشعيع بالكوبالت بالانخفاض في قيم الجهد والتيار والطاقة الناتج عن تشعيع الخلية الثانية بالسيزيوم وجد أن



الانخفاض في قيمة الجهد للخلية الاولى يفوق الانخفاض في قيمة الجهد للخلية الثانية ب 0.04% ,  
% 0.0001 0.001% علي التوالي , كما وجد أن الانخفاض في قيم التيار للخلية الاولى يفوق  
الانخفاض في قيمة التيار للخلية الثانية ب 1.96% , 2% , 4.9% علي التوالي . وبالمثل وجد أن  
الانخفاض في قيمة الطاقة للخلية الاولى يفوق الانخفاض في قيمة الطاقة للخلية الثانية ب 2%  
1.9% 4.7% علي التوالي .

بهذا فقد اكدت النتائج تأثير أشعة غاما علي تدهور جودة أداء الخلايا الشمسية السيليكونية , كما أكدت  
إرتباط هذا التأثير بكمية الجرعة الإشعاعية التي تستقبلها الخلية الشمسية .

# TABLE OF CONTENTS

<i><b>NO.</b></i>	<i><b>Title</b></i>	<i><b>PAGE NO.</b></i>
	<i>Alaya</i>	
	<i>Dedication</i>	<b>I</b>
	<i>Acknowledgements</i>	<b>II</b>
	<i>Abstract (English)</i>	<b>III</b>
	<i>Abstract (Arabic)</i>	<b>VI</b>
	<i>Contents</i>	<b>VII</b>
	<i>List of figures</i>	<b>X</b>
	<i>List of tables</i>	<b>XIII</b>
	Chapter one Introduction	
<b>1.1</b>	Introduction	<b>1</b>
<b>1.2</b>	Statement Of The Problem	<b>2</b>
<b>1.3</b>	Previous Studies	<b>3</b>
<b>1.4</b>	Hypothesis Of Research	<b>5</b>
<b>1.5</b>	Objectives Of The Research	<b>6</b>
<b>1.6</b>	Significance Of The Research	<b>7</b>
<b>1.7</b>	Methodology	<b>8</b>
	Chapter Two Literature Review	
<b>2.1</b>	Introduction	<b>9</b>
<b>2.2</b>	Nature of Radiation	<b>9</b>
<b>2.3</b>	Types of Ionizing Radiation	<b>10</b>
<b>2.3.1</b>	Alpha Particles	<b>10</b>
<b>2.3.2</b>	Beta Particles	<b>12</b>
<b>2.3.3</b>	Gamma Rays	<b>14</b>
<b>2.4</b>	Sources of Gamma Ray	<b>15</b>
<b>2.5</b>	Gamma Interaction With Matter	<b>15</b>

<b>2.6</b>	Types Of Interaction Of Gamma Radiation With Matter	<b>16</b>
<b>2.6.1</b>	Photoelectric Effect	<b>16</b>
<b>2.6.2</b>	Compton Scattering	<b>16</b>
<b>2.6.3</b>	Pair Production	<b>18</b>
<b>2.7</b>	Radiation Damage In Silicon	<b>19</b>
	<b>Chapter Three</b> <b>Radiation Damage On Solar Cells</b>	
<b>3.1</b>	Introduction	<b>22</b>
<b>3.2</b>	Operation Principles Of Solar Cells	<b>22</b>
<b>3.3</b>	Displacement Damage	<b>26</b>
<b>3.4</b>	Gamma Displacement Cross-Section	<b>27</b>
<b>3.4.1</b>	Photoelectric Effect Displacement Cross-Section	<b>27</b>
<b>3.4.2</b>	Compton Scattering Effect Displacement Cross-Section	<b>28</b>
<b>3.4.3</b>	Pair Production Effect Displacement Cross-Section	<b>29</b>
<b>3.5</b>	Radiation Damage In Solar Cells	<b>30</b>
	<b>Chapter Four</b> <b>Experimental Measurements</b>	
<b>4.1</b>	Introduction	<b>32</b>
<b>4.2</b>	Gamma Ray Displacement Damage	<b>33</b>
<b>4.3</b>	Effect Of Displaced Atoms On Solar Cell Performance	<b>34</b>
<b>4.4</b>	Instruments	<b>34</b>
<b>4.5</b>	Measurements Procedure	<b>42</b>
	<b>Chapter Five</b> <b>Results And Discussions</b>	
<b>5.1</b>	Introduction	<b>45</b>
<b>5.2</b>	Effects Of $^{60}\text{Co}$ $\gamma$ -ray Irradiation On The I-V And P-V Characteristics	<b>45</b>
<b>5.3</b>	Effects Of $^{60}\text{Co}$ $\gamma$ -ray Irradiation On The $V_{oc}$ , $I_{sc}$ FF, $\eta$	<b>50</b>
<b>5.4</b>	Effects Of $^{137}\text{Cs}$ $\gamma$ -ray Irradiation On The I-V And P-V Characteristics	<b>54</b>
<b>5.5</b>	Effects Of $^{137}\text{Cs}$ $\gamma$ -ray Irradiation On The $V_{oc}$ , $I_{sc}$ FF, $\eta$	<b>58</b>
<b>5.6</b>	Comparison Between The Illumination Of $^{60}\text{Co}$ $\gamma$ -ray and $^{137}\text{Cs}$ $\gamma$ -ray Irradiation On The I-V And P-V Characteristics	<b>60</b>
<b>5.7</b>	Conclusion	<b>68</b>
<b>5.8</b>	Recommendations	<b>70</b>
	References	<b>72</b>

## List of Figures

NO.	TITLE	PAGE NO.
	<b>Chapter one</b> <b>Introduction</b>	
<b>1.1</b>	A Solar Power System Integrated With A Space Probe	<b>5</b>
	<b>Chapter Two</b> <b>Basic Contents</b>	
<b>2.1</b>	Sketch Diagram For Alpha Particle Emission	<b>11</b>
<b>2.2.(a)</b>	Sketch Diagram For Beta Minus Emission	<b>12</b>
<b>2.2.(b)</b>	Sketch Diagram For Positron Emission	<b>13</b>
<b>2.3</b>	Sketch Diagram For Gamma Emission	<b>14</b>
<b>2.4</b>	Displacement Damage Cross Section As A Function Of Gamma Energy For Silicon	<b>21</b>
	<b>Chapter Three</b> <b>Radiation Damage On Solar Cells</b>	
<b>3.1</b>	A Schematic Drawing Of A Single Junction Solar Cell	<b>23</b>
<b>3.2</b>	Typical I-V Curves Measured On A Single Junction Solar Cell	<b>25</b>
	<b>Chapter Four</b> <b>Experimental Measurements</b>	
<b>4.1</b>	Schematic Diagram For The Circuit Utilized For Measurements	<b>35</b>
<b>4.2</b>	A Photograph For The (Light-Solar Cell) Geometry	<b>36</b>
<b>4.3</b>	A Photograph For The (Light-Solar Cell) Geometry During Gamma Exposure	<b>39</b>
<b>4.4</b>	A Photograph of a Solar Cell analyzer type HT300 used to measure the light intensity	<b>40</b>
<b>4.5</b>	A Photograph Of A Pyranometer Type HT303N Used To Measure The Light Intensity	<b>41</b>
	<b>Chapter Five</b> <b>Results, Discussions and Conclusion</b>	

<b>5.1</b>	The illuminated I-V characteristics of mi-solar cell irradiated with 1.25 Mev <sup>60</sup> Co photons at various doses collectively	<b>48</b>
<b>5.2</b>	The illuminated P-V characteristics of mi-solar cell irradiated with 1.25 Mev <sup>60</sup> Co photons at various doses collectively	<b>49</b>
<b>5.3</b>	Variation of normalized V <sub>oc</sub> , and I <sub>sc</sub> with <sup>60</sup> Co gamma exposure doses	<b>52</b>
<b>5.4</b>	Variation of normalized FF, and η with <sup>60</sup> Co gamma exposure doses	<b>53</b>
<b>5.5</b>	The illuminated I-V characteristics of mi-solar cell irradiated with 0.662 Mev <sup>137</sup> Cs photons at various doses collectively	<b>56</b>
<b>5.6</b>	The illuminated P-V characteristics of mi-solar cell irradiated with 0.662 Mev <sup>137</sup> Cs photons at various doses collectively	<b>57</b>
<b>5.7.a</b>	The illuminated I-V characteristics of mi-solar cell irradiated with 532 mR <sup>60</sup> Co gamma photons VS 280 mR <sup>137</sup> Cs gamma photons	<b>62</b>
<b>5.7.b</b>	The illuminated I-V characteristics of mi-solar cell irradiated with 1064 mR <sup>60</sup> Co gamma photons VS 560 mR <sup>137</sup> Cs gamma photons	<b>63</b>
<b>5.7.c</b>	The illuminated I-V characteristics of mi-solar cell irradiated with 1596 mR <sup>60</sup> Co gamma photons VS 837 mR <sup>137</sup> Cs gamma photons	<b>64</b>
<b>5.8.a</b>	The illuminated P-V characteristics of mi-solar cell irradiated with 532 mR <sup>60</sup> Co gamma photons VS 280 mR <sup>137</sup> Cs gamma photons	<b>65</b>
<b>5.8.b</b>	The illuminated P-V characteristics of mi-solar cell irradiated with 1064 mR <sup>60</sup> Co gamma photons VS 560 mR <sup>137</sup> Cs gamma photons	<b>66</b>
<b>5.8.c</b>	The illuminated P-V characteristics of mi-solar cell irradiated with 1596 mR <sup>60</sup> Co gamma photons VS 837 mR <sup>137</sup> Cs gamma photons	<b>67</b>

## List of Tables

NO.	Title	PAGE NO.
<b>5.1</b>	The illuminated I-V and P-V values of mi-solar cell irradiated with 1.25 Mev <sup>60</sup> Co photons at various doses collectively	<b>47</b>
<b>5.2</b>	The illuminated I-V and P-V values of mi-solar cell irradiated with 0.662 Mev <sup>137</sup> Cs photons at various doses collectively	<b>51</b>
<b>5.3</b>	Variation of normalized $V_{oc}$ , $I_{sc}$ ,FF, and $\eta$ with <sup>60</sup> Co gamma exposure doses	<b>55</b>
<b>5.5</b>	Variation of normalized $V_{oc}$ , $I_{sc}$ ,FF, and $\eta$ with <sup>137</sup> Cs gamma exposure doses	<b>59</b>

# Chapter One

## Introduction

### 1.1. Introduction

Many different semiconductor materials can potentially be used to make solar cells. However, when a high efficiency is required, the choice of the material becomes restricted to Si, GaAs, InP and GaInP alloys and related hetero structures. This is because only these materials can be grown with a good crystalline quality, controlled impurity content and a large enough lifetimes. Si, GaAs and GaInP possess also the overwhelming advantage of a sufficiently well-mastered technology. The study of radiation induced degradation of solar cells, being in practice only interesting for space applications, is of course restricted to the high-efficiency materials. For this reason, in the research involved in this work, we only consider the defects induced in Si-based solar cells currently used to make space solar power systems. Mono-crystalline silicon (mc-Si) solar cell is a part of silicon based solar cell family and one of the first developed and mostly used solar cells because it has a number of advantages like low maintenance cost, high reliability, noiseless and eco-friendly [1,2]. Conventional mc-Si solar cells generally exhibit good spectral response to visible radiation, which occupies the 400-800 nm wavelength region of the electromagnetic spectrum.

However, mc-Si solar cells are extremely sensitive to high-level radiation such as  $^{60}\text{Co}$  and  $^{137}\text{Cs}$   $\gamma$ -ray photons. Several studies have reported the degradation of photovoltaic parameters for mc-Si solar cells under  $^{60}\text{Co}$   $\gamma$ -irradiation [3,4]. For this we recall the mechanism of defect production in these semiconductor materials by gamma photon irradiation. The defects are to be evaluated by carrying out experimental measurements and to evaluate the Direct Ionizing Radiation Damage by evaluating the I-V characteristics of the solar units under test.

## **1.2. Statement of the Problem**

Solar cells are the basis of nearly all space power systems. The space market for commercial communications as well as military and scientific applications is driving a rapid development of new solar cells technologies to provide increased power.

However, the space environment is a dynamic mixture of different space energetic particles, these particles enter the space solar cells and cause defects as they pass through and are slowed down. These defects can lead to a possible degradation of the electrical performance of the solar cell, which could have negative impact on both the financial and environmental aspects of the solar cell application.



This work is exploring such effects by addressing the impact of  $^{60}\text{Co}$  and  $^{137}\text{Cs}$  gamma-ray photons on the electrical performance of mono-crystalline silicon solar cells.

### **1.3 Previous Studies**

During the previous decades, many researchers tested various optoelectronic devices and published the results of their researches [3–10].

R.J.Walters and S.R.Messenger showed that when irradiating InP solar cells with charged particles (1MeV electron, 3MeV proton), changes in diffusion current occurs. Junga FA and Enslow GM concluded that any change in carriers lifetime and mobility due to irradiation of gamma photons and neutrons will affect the performance of silicon solar cells. Moreover R.Radosavljevic and A.Vasic showed that the output current and output power of solar cells decreases when the solar cell gets exposed to different radiation environments.

When gamma rays interact with material, two types of radiation damage effects occur, displacement damage and ionization effects.

Ionization effect is the generation of electron-hole pairs within the material which can be caused by either Photoelectric effect, Compton scattering, or pair production where they eject electrons from the atoms of the material.

These ejected electrons can create secondary reactions. The result is a track of ionized atoms in the bulk of the material. The second effect is atomic displacement which is known as the movement of atoms from their normal position in the lattice to another placement, causing a defect in the lattice

material.

Sometimes the atom receives so much kinetic energy at the site of interaction that it leaves its initial location in the material. This displacement creates additional atomic movement on its track that may result in a cluster of defects into the atomic lattice. The immediate and long-term results of ionization and atomic displacement strongly depend on the material.

After electron-hole generations, electrons and holes travel in the bulk under the influence of the local electric field.

The mobility of electrons is much higher than the mobility of holes, but both charge carriers may get into defects of the lattice called traps. Charge carriers accumulate around traps and create a local charge build-up. These traps can be single point defects or a mismatch of interface surfaces [11,12]. High-energy photons give rise to clusters of defects and low-energy photons only produce single point defects. The interstitial atoms are not such electrically active as a complex of defects. Defects introduce intermediate energy levels in the gap between the conducting band and the valence band. These band-gap defects disturb the transport of electrical charges by several reactions [13].

First, generation and recombination of electron-hole pairs degrade the minority carrier lifetime. Second, the trapping and compensation effects change the majority carrier density and decrease the carrier mobility [14].

The results show that, under the influence of these effects, the reduction of photocurrent is significant. In this work,  $^{60}\text{Co}$  and  $^{137}\text{Cs}$  are used to irradiate a silicon-based solar cell, to evaluate the impact of such gamma photons on the

electrical properties including the output power.

Figure 1.1 shows a photo for a solar power system integrated with a space probe.



Fig1.1, A solar power system integrated with a space probe.

#### **1.4. Hypothesis of Research**

$\gamma$  radiation damage is induced by the ionization and excitation of the atoms within the junction space charge region of a junction device such as solar cell. The presence of impurity atoms that are either added to the base material as donors, or during the manufacturing process, has indicated the possibility that

some of the produced electrons might be trapped by those atoms between the valence and conduction band. Consequently, the output of the optoelectronic device exposed to  $\gamma$  radiation is also reduced. Therefore, from the technological point of view, it is important to study the variations induced by irradiation of semiconductor junction characteristic parameters that affect the performance of the solar cells [15-20].

During inelastic scattering on electrons, the incident particle can transfer energy to the atom, raising it to a higher energy level (excitation), or it may transfer enough energy to remove an electron from the atom (ionization).

A portion of energy transferred during each individual scattering of heavy charged particles on electrons is small compared to an entire kinetic energy of a particle, but the number of particle collisions per a unit path length is as high that the entire total energy loss is significant even in relatively thin material layers.

### **1.5. Objectives of the Research**

All presented publications give a substantial insight into the state of the art concerning this important interdisciplinary field. Comprehensive comparative analysis of measurement results were carried out in order to determine the reliability of optoelectronic devices in radiation environment, [3-13].

This work, studies the basic physical mechanisms of the interactions of ionizing radiation with solar cells targeting the radiation-induced effects generated by gamma ray photons of  $^{60}\text{Co}$  and  $^{137}\text{Cs}$  gamma ray source.

These defects are to be evaluated by carrying out experimental measurements and to evaluate the Direct Ionizing Radiation Damage by evaluating the I-V characteristics of the solar units under test.

## **1.6. Significance of the Research**

Beside the diversity of the device technologies used for designing the solar cells and various optoelectronic devices, there are a variety of radiation environments in which they are used (natural space and atmospheric, as well as military and civil nuclear environments, etc.).

Reliability of electrical devices in a radiation environment is very important, and extensive studies concerning the development of semiconductor devices that can operate normally in such conditions have been seriously undertaken.

Possible degradation of the electrical performance of optoelectronic devices in general, induced by irradiation, means that very strict conditions for their application must be predetermined for the worst-case scenario. Performance failure in such conditions could have negative impact on both the financial and environmental aspects of the device application.

The significance of the current study relies on its contribution to the efforts being done to study the radiation-induced effects on the electrical properties of solar cells and to develop a radiation-hardened electronics for solar power systems working in radiation environment, [21-24].

## 1.7. Methodology

For this experimental study a suitable (light source - solar cell) geometry will be instrumented individually for both  $^{60}\text{Co}$  and  $^{137}\text{Cs}$  radioactive sources which will be used individually to expose monocrystalline silicon solar cells. Each geometry consists of a halogen lamp, and a mono-crystalline silicon solar cell. At room temperature, the forward bias (I-V) and (P-V) characteristics will be determined under illumination, before and after  $\gamma$ - irradiation.

The first solar cell will be irradiated with different  $^{60}\text{Co}$   $\gamma$ -exposure doses , for different periods of time . The second solar cell will be irradiated with different  $^{137}\text{Cs}$   $\gamma$ -exposure doses; for different periods of time. The current–voltage characteristics of each mono-crystalline silicon solar cell under AM1.5 illumination condition and their spectral photocurrent will be studied before and after gamma irradiation. The results would be analyzed using sigma plot program, which is a proprietary software for scientific graphing and data analysis. It can read multiple formats such as Microsoft Excel spread sheets and can perform mathematical transforms and statistical analysis. Then the results of  $^{60}\text{Co}$  exposure will be studied and compared to those of  $^{137}\text{Cs}$  radiation.

# **Chapter Two**

## **Basic contents**

### **2.1. Introduction**

Radiation in space is generated by particles emitted from a variety of sources both within and beyond our solar system. Radiation effects from these particles can not only cause degradation, but can also cause failure of electronic and electrical system in space vehicles or satellites,[25] .Galactic cosmic rays are one of the most important barriers standing in the way of plans for interplanetary travel by crewed spacecraft; they also pose a threat to electronics placed aboard outgoing probes. In 2010, a malfunction aboard the Voyager 2 space probe was credited to a single flipped bit, probably caused by a cosmic ray. [26],[27]. In this thesis we are interested in knowing how radiation can affect solar cells performance, therefore we must know more about radiation.

### **2.2. Nature of Radiation**

Radiation is energy that comes from a source and travels through space and may be able to penetrate various materials. Interestingly, there is a "background" of natural radiation everywhere in our environment. Ubiquitous background radiation comes from space (i.e., cosmic rays) and from naturally occurring radioactive materials contained in the earth and in living things.

There are two different kinds of radiation: Ionizing radiation, Non-ionizing

radiation. Ionizing radiation is produced by unstable atoms which have an excess of energy, mass or both. Atoms with unstable nuclei are said to be radioactive.

In order to reach stability, these atoms give off, or emit, the excess energy or mass. These emissions are called radiation which can be delivered in form of electromagnetic waves (like light) or particulate (i.e., mass given off with the energy of motion) [28]. In this study we are more concerned about ionizing radiation because it is more energetic than non-ionizing radiation, and it has so much energy that it can knock electrons out of atoms.

## **2.3. Types of Ionizing Radiation**

### ***2.3.1. Alpha Particles***

Alpha particles ( $\alpha$ ) are emitted by some unstable atoms. They are positively charged and made up of two protons and two neutrons from the atom's nucleus. Alpha particles come from the decay of the heaviest radioactive elements, such as uranium, radium and polonium. Even though alpha particles are very energetic, they are so heavy that they use up their energy over short distances and are unable to travel very far from the atom.

The health effect from exposure to alpha particles depends greatly on how a



person is exposed. Sketch diagram is shown in figure (2.1).

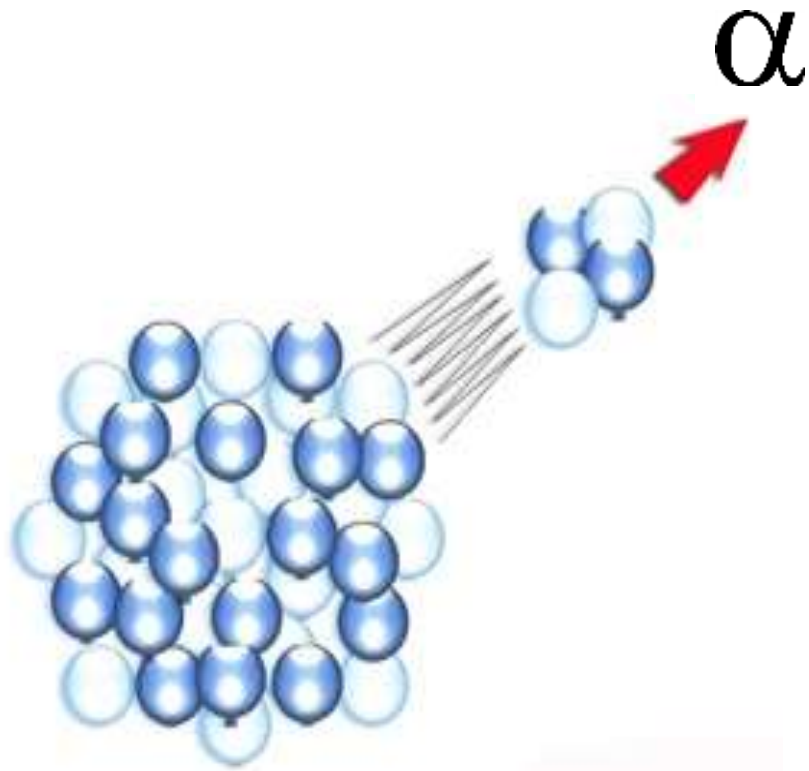


**Fig.2.1, Sketch diagram for Alpha particle emission**

### ***2.3.2. Beta Particles***

Beta particles ( $\beta$ ) are small, fast-moving particles with a negative electrical charge ( $\beta^-$ -particles) or positive electrical charge ( $\beta^+$ -particles) that are emitted from an atom's nucleus during radioactive decay.

These particles are emitted by certain unstable atoms such as hydrogen-3 (tritium), carbon-14 and strontium-90. Sketch diagram is shown in figure 2.2. (a),(b).

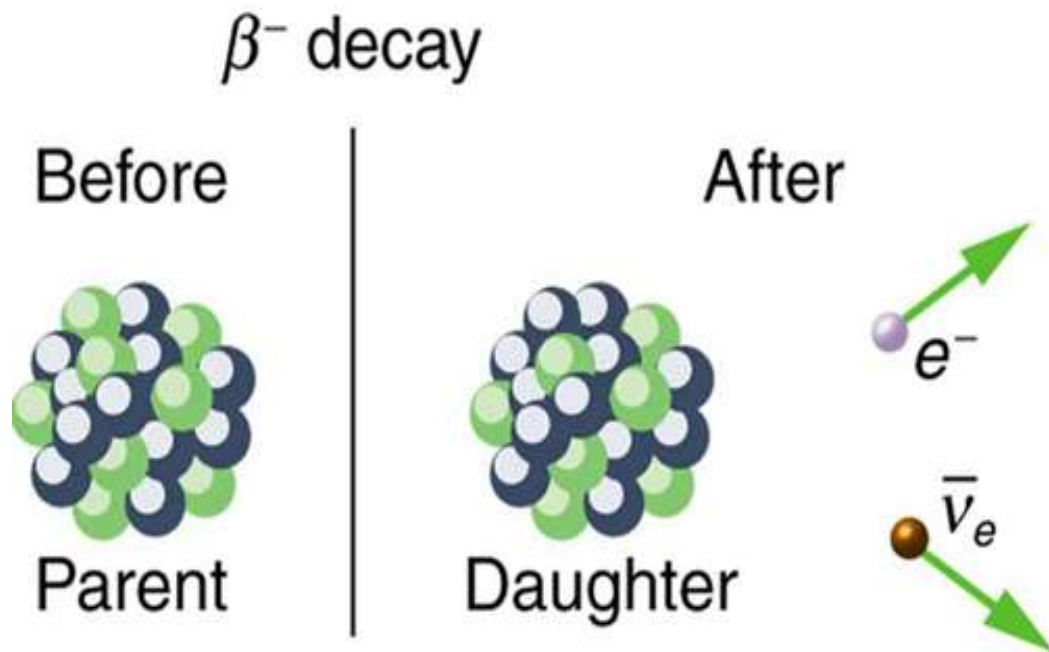


**Fig.2.2.(a), Sketch diagram for Beta minus emission**

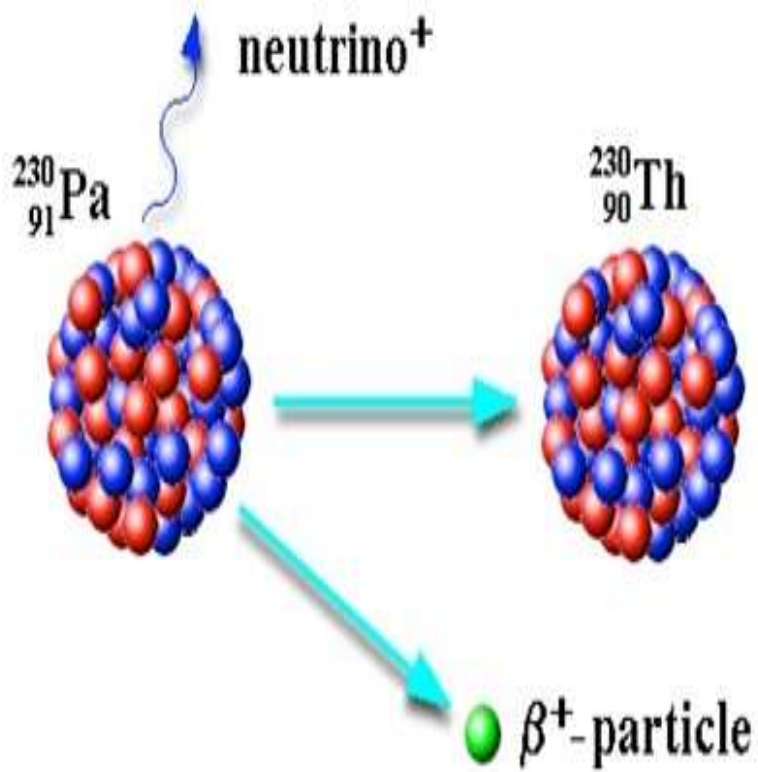


**Fig.2.2.(b),Sketch diagram for positron emission**

### 2.3.3. Gamma Rays

Gamma rays are high-energy electromagnetic radiation emitted in the de excitation of the atomic nucleus.[29] . Unlike alpha and beta particles, which have both energy and mass, gamma rays are pure energy. They are similar to visible light, but have much higher energy.

Gamma rays are classically produced by the decay from high energy states of atomic nuclei (gamma decay), but can also be created by other processes. Gamma rays were first thought to be particles with mass, like alpha and beta rays. Rutherford initially believed they might be extremely fast beta particles, but their failure to be deflected by a magnetic field indicated they had no charge. Sketch diagram is shown in figure 2.3.

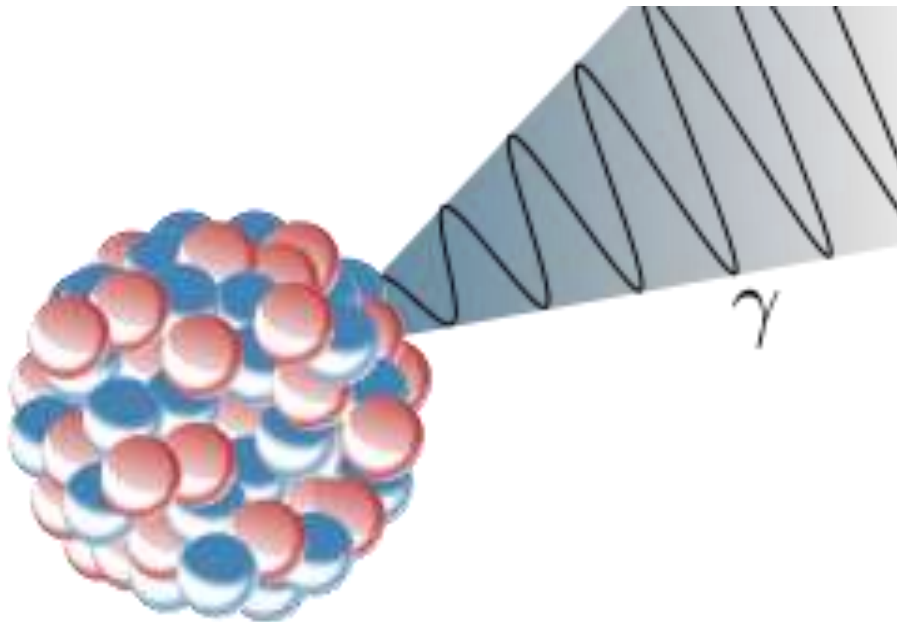


**Fig.2.3, Sketch diagram for gamma emission**

## 2.4. Sources of gamma rays

Natural sources of gamma rays on Earth include gamma decay from naturally occurring radioisotopes such as potassium-40, and also as a secondary radiation from various atmospheric interactions with cosmic ray particles. Some rare terrestrial natural sources that produce gamma rays that are not of a nuclear origin, are lightning strikes and terrestrial gamma-ray flashes, which produce high energy emissions from natural high-energy voltages. Gamma rays are also produced by a number of astronomical processes in which very high-energy electrons are produced. Such electrons produce secondary gamma rays by the mechanisms of bremsstrahlung, inverse Compton scattering and synchrotron radiation. Among the commonly used radioisotopes as gamma sources are; Co-60, Cs-137,[29].

## 2.5. Gamma interaction with matter

When a gamma ray passes through matter, the probability for absorption is proportional to the thickness of the layer, the density of the material, and the absorption cross section of the material. The total absorption shows an exponential decrease of intensity with distance from the incident surface;

$$I(x) = I_0 \cdot e^{-\mu x} \quad (2.1)$$

where  $x$  is the distance from the incident surface,  $\mu = n\sigma$  is the absorption coefficient, measured in  $\text{cm}^{-1}$ ,  $n$  the number of atoms per  $\text{cm}^3$  of the material

(atomic density) and  $\sigma$  the absorption cross section in  $\text{cm}^2$  [30].

## **2.6. Types of Interaction of Gamma Radiation with Matter**

Gamma radiation ionizes materials via three processes: the photoelectric effect, Compton scattering, and pair production.

### ***2.6.1. Photoelectric effect***

This describes the case in which a gamma photon interacts with and transfers its energy to an atomic electron, causing the ejection of that electron from the atom. The kinetic energy of the resulting photoelectron is equal to the energy of the incident gamma photon minus the energy that originally bound the electron to the atom (binding energy). The photoelectric effect is the dominant energy transfer mechanism for X-ray and gamma ray photons with energies below 50 keV (thousand electron volts), but it is much less important at higher energies.

### ***2.6.2. Compton scattering***

Compton scattering is an example of elastic scattering of light by a free charged particle, where the wavelength of the scattered light is different from that of the incident radiation.

In Compton's original experiment, the energy of the X ray photon ( $\approx 17\text{keV}$ ) was very much larger than the binding energy of the atomic electron, so the electrons could be treated as being free. The amount by which the light's wavelength changes is called the Compton shift. Although nuclear Compton scattering exists,[31], Compton scattering usually refers to the interaction involving only the electrons of an atom. The Compton Effect was observed by Arthur Holly Compton in 1923 at Washington University in St. Louis and further verified by his graduate student Y. H. Woo in the years following. Compton earned the 1927 Nobel Prize in Physics for the discovery.

The effect is important because it demonstrates that light cannot be explained purely as a wave phenomenon. Thomson scattering, the classical theory of an electromagnetic wave scattered by charged particles, cannot explain low intensity shifts in wavelength (classically, light of sufficient intensity for the electric field to accelerate a charged particle to a relativistic speed will cause radiation-pressure recoil and an associated Doppler shift of the scattered light, [32], but the effect would become arbitrarily small at sufficiently low light intensities regardless of wavelength). Light must behave as if it consists of particles, if we are to explain low-intensity Compton scattering. Compton's experiment convinced physicists that light can behave as a stream of particle-like objects (quanta), whose energy is proportional to the light wave's frequency.

Because the mass-energy and momentum of a system must both be conserved, it is not generally possible for the electron simply to move in the direction of the incident photon.

The interaction between electrons and high energy photons (comparable to the rest energy of the electron, 511 Kev) results in the electron being given part of the energy (making it recoil), and a photon of the remaining energy being emitted in a different direction from the original, so that the overall momentum of the system is conserved. If the scattered photon still has enough energy, the process may be repeated. In this scenario, the electron is treated as free or loosely bound.

### ***2.6.3. Pair production***

This becomes possible with gamma energies exceeding 1.02 MeV, and becomes important as an absorption mechanism at energies over 5 MeV. By interaction with the electric field of a nucleus, the energy of the incident photon is converted into the mass of an electron-positron pair. Any gamma energy in excess of the equivalent rest mass of the two particles (totaling at least 1.02 MeV) appears as the kinetic energy of the pair and in the recoil of the emitting nucleus.



At the end of the positron's range, it combines with a free electron, and the two annihilate, and the entire mass of these two is then converted into two gamma photons of at least 0.51 MeV energy each (or higher according to the kinetic energy of the annihilated particles, [33]).

## 2.8. Radiation Damage In Silicon

It has been assumed that the radiation damage in silicon is proportional to the energy deposited into the displacement interactions (NIEL hypothesis), [30].

The displacement damage cross section  $D(E_p)$  expresses the relative displacement efficacy of an impinging particle  $p$  with energy  $E_p$ , taking into account the various type of interactions between the particle and the silicon atom. The displacement damage cross section is defined by [34]:

$$D(E_P) = \sum_i \sigma_i(E_P) \int_{E_{Rmin}}^{E_{Rmax}} d E_R f_i(E_P, E_R) P(E_R) \quad (2-2)$$

The function  $f_i$  describes the distribution of the recoil atom with energy  $E_R$  and  $P(E_R)$  is the Lindhard partition function of the energy loss in non-ionizing processes by a recoiling nucleus of energy  $E_R$ . The lower bound of the integral corresponds to the minimum energy required to displace a silicon atom from the lattice and the upper limit is determined by the maximum energy transferred.

The gamma displacement cross-sections for energies up to 14 MeV have been calculated in various materials at two values of displacement threshold energy (24 and 40 eV), [35]. Three types of gamma ray interactions with materials were considered, the photoelectric effect, Compton scattering and pair production. Therefore, the total gamma displacement cross-section consists of three components representing the sum of cross-sections for three interactions;

$$\sigma_{\gamma}^T(E_{\gamma}) = \sigma_{\gamma}^{PE}(E_{\gamma}) + \sigma_{\gamma}^{CS}(E_{\gamma}) + \sigma_{\gamma}^{PP}(E_{\gamma}) \quad (2-3)$$

Where  $E_{\gamma}$  is the gamma incident energy and the superscripts PE, CS, and PP represent photoelectric effect, Compton scattering, and pair production, respectively. Using the data obtained in [35], the total displacement damage cross section of silicon for photons is presented in Fig.2.4.

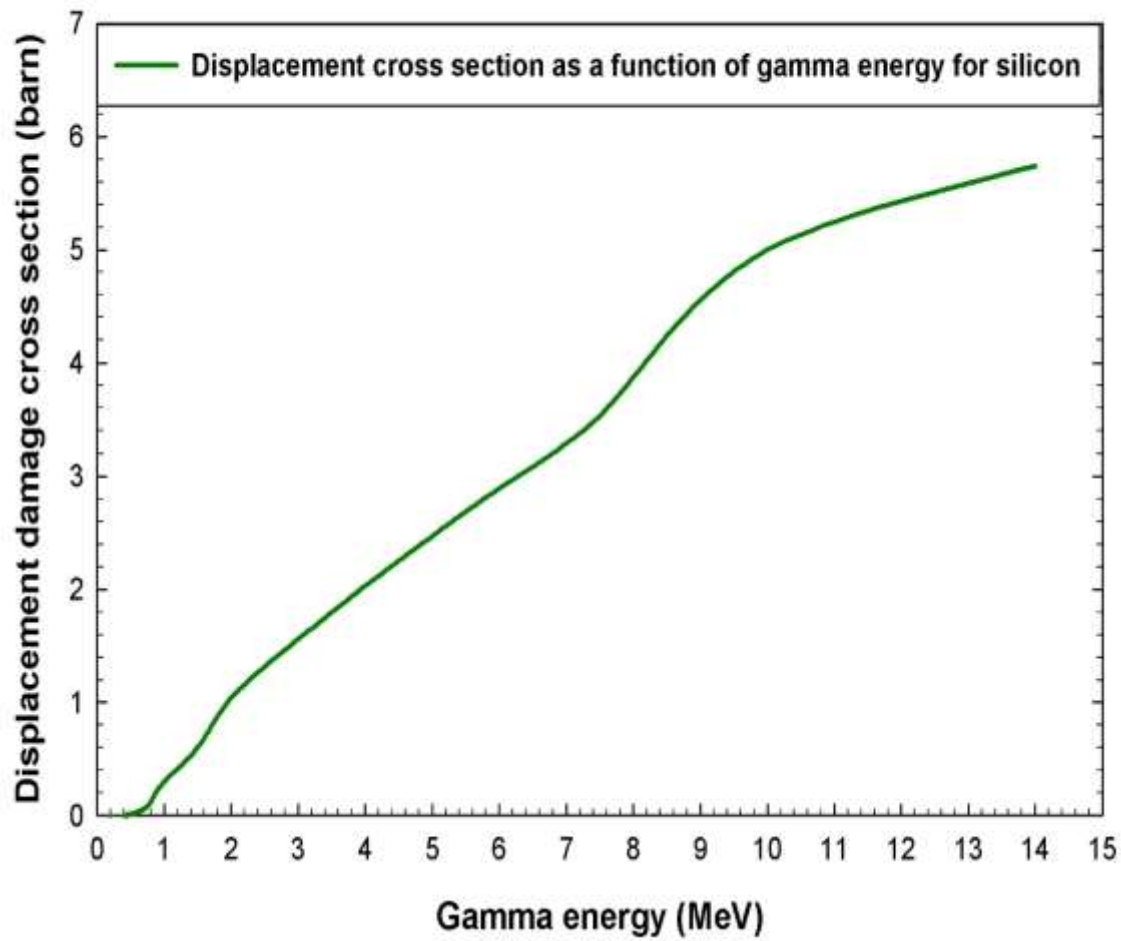


**Figure 2.4. Displacement damage cross section as a function of gamma energy for silicon**

## **Chapter Three**

### **Radiation damage on solar cells**

#### **3.1. Introduction**

As worldwide energy demand increases, conventional energy resources will be exhausted in the not-too-distant future. Therefore the solar cell is the major candidate for obtaining energy from sun, since it can provide nearly permanent power at low operating cost and almost free of pollution. Solar cells at present furnish the most important long-duration power supply for satellites and space vehicles and have also been successfully employed in terrestrial applications.

The space environment is often characterized by a rich radiation environment; therefore, to be used in space, the radiation response of a solar cell must be well understood.

#### **3.2. Operating principles of solar cells**

A solar cell consists essentially of a **p-on-n** junction in a semiconductor material that, when under illumination by solar photons, produces a voltage, called the photovoltage, by the photovoltaic effect. If an ohmic contact is placed on **p** and **n** sides of the junction, then the photogenerated charge carriers can be extracted from the device, thus generating a photocurrent. If the solar cell is connected across an electronic load, then power can be extracted and used to drive a system.

A schematic drawing of a basic, single-junction solar cell is shown in Figure (3.1) .this figure depicts an n+p structure where the n-type dopant concentration is one or two orders of magnitude higher than that of the p-type region so that a one-sided, abrupt junction exists. When the solar cell is illuminated, the photons penetrate the material, and those photons with energy above the semiconductor band gap are absorbed and create electron-hole pairs[36].

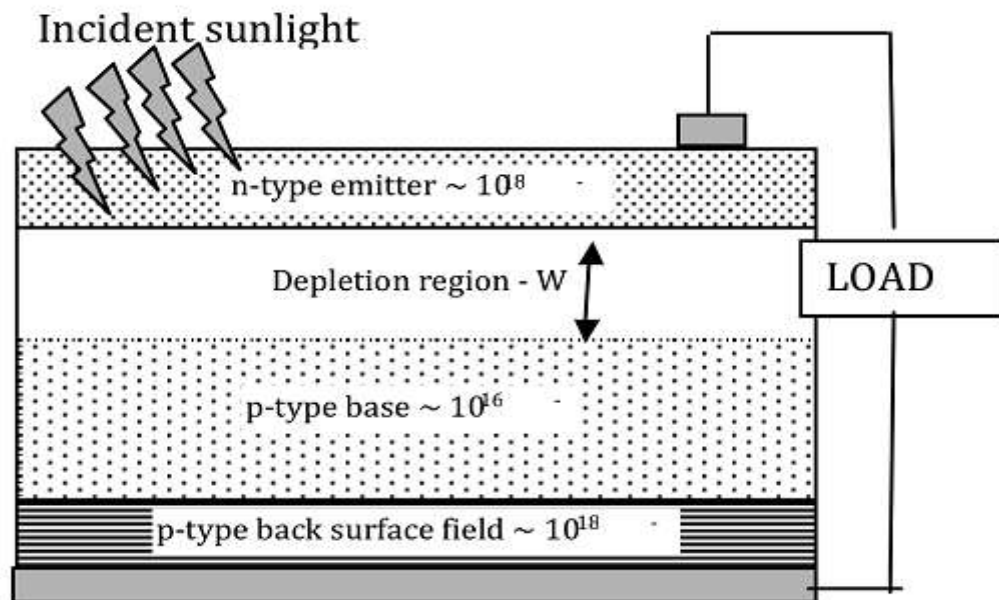


**Figure 3.1: A schematic drawing of a single junction solar cell.**

The electrical output of a solar cell is typically characterized by parameters extracted from the IV curve. Three common parameters are illustrated in Figure 3.2. The current measured at short circuit is called the short circuit current ( $I_{sc}$ ). The voltage at open circuit is called the open circuit voltage ( $V_{oc}$ ). The maximum electrical power generated by the solar cell is given the symbol  $P_{mp}$ . The efficiency at which the solar cell converts the incident solar energy to electrical energy is given by dividing  $P_{mp}$  by the appropriate solar constant, which, for the space air mass zero (AM0) spectrum, is  $136.7 \text{ mW/cm}^2$ .

The shape of the IV curve is characterized by the fill factor (FF). The FF is defined as the ratio of  $P_{mp}$  to the product of  $I_{sc}$  and  $V_{oc}$ . The FF gives an indication how well the IV curve fills the maximum power rectangle, which is the rectangle formed in the fourth quadrant by a vertical line passing through  $V_{oc}$  and an horizontal line passing through  $I_{sc}$  as shown by the dotted lines in Figure (3.2)[36]. The performance of a solar cell is also characterized in terms of the solar cell dark IV curve.

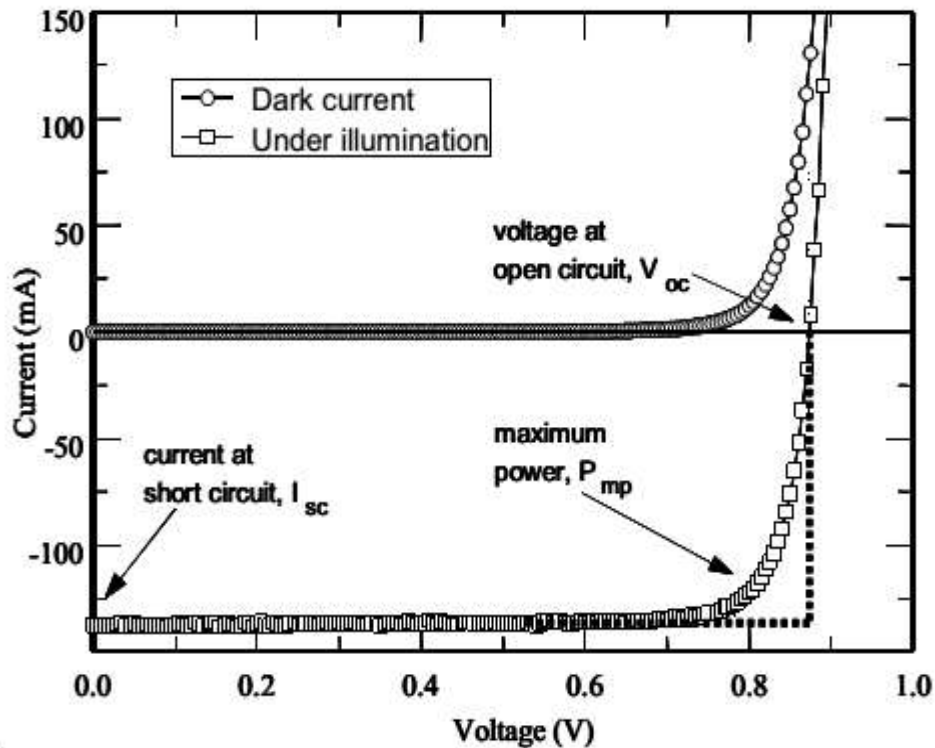


**Figure 3.2: Typical IV , PV curves measured on a single-junction solar cell.**

As seen in figure 3.2, Illuminating the solar cell pulls the IV curve down into the forth quadrant so that power can be extracted from the device. The dark current is seen to oppose the photo generated current. Typical parameters used to characterize solar cell performance are shown. The dotted lines define the “maximum power rectangle”.

### 3.3. Displacement damage

The electrical characteristics of silicon solar cells are affected by environment condition. During operation of photovoltaic solar cells, they are exposed to radiation such as used in space systems and satellites.

The irradiation of solar cells by high-energy levels of radiation in the form of gamma rays, neutrons, charged particles, etc. leads to radiation defects and electrical damage in the solar cells bulk and results a significant degradation of the electrical parameters of silicon solar cells [37,39].

The lifetime and performance of the solar cells is limited by the amount of radiation damage in solar cells. When silicon solar cells are irradiated with gamma rays, two types of radiation damage occur within it: displacement damage and ionization effects. These defects mostly act as recombination points that decreased the diffusion length and lifetime of minority carrier as well as increased internal parameters of cells. Output parameters of solar cell such as maximum output power, fill factor, efficiency, short circuit current, and open circuit voltage strongly depend on internal parameters of solar cells such as series resistance,  $R_s$ , saturation current,  $I_0$  and ideal factor,  $n$ . it has been proved that increasing each of above internal parameters of solar cell causes that the output characteristics of solar cells decreased [39-41].



### 3.4. Gamma displacement cross-sections

Gamma rays can displace atoms by first transferring energy to an electron, which transfers energy to a lattice atom through an electron-atom scattering event. The energetic electrons can be produced from Compton scattering, photoelectric effect and pair production.

Therefore, the total gamma displacement cross-section consists of three components representing the sum of cross-sections for three interactions,

$$\sigma_{\gamma}^{\text{T}}(E_{\gamma}) = \sigma_{\gamma}^{\text{PE}}(E_{\gamma}) + \sigma_{\gamma}^{\text{CS}}(E_{\gamma}) + \sigma_{\gamma}^{\text{PP}}(E_{\gamma}) \quad (3-1)$$

Where  $E_{\gamma}$  is the gamma incident energy and the superscripts PE, CS, and PP represent photoelectric effect, Compton scattering, and pair production, respectively.

#### 3.4.1. Photoelectric effect displacement cross-section

For gamma ray energies below 0.1 MeV, the dominant mode of interaction of the gamma ray with material is the photoelectric effect. In this process, a gamma ray is absorbed by an atom and then an energetic photoelectron is ejected from one of its bound shells. The ejected electron possesses kinetic energy  $E_0$ , which is equal to the incident gamma energy  $E_{\gamma}$  minus the binding energy (BE) of the electron to the atom.

Under the assumption that all electrons have the same initial energy for the given gamma energy of  $E_\gamma$  resulting from K-shell ionization, the photoelectric effect displacement cross-section is given by:

$$\sigma_\gamma^{\text{PE}}(E_\gamma) = \sigma^{\text{PE}}(E_\gamma, E_0) \cdot \bar{n}(E_0) \quad (2-3) \quad (3.2)$$

Where  $\bar{n}(E_0)$  is the total number of displaced atoms produced on the average over the range of the recoil electron of energy  $E_0$ .

### ***3.4.2. Compton scattering displacement cross-section***

Compton scattering takes place between the incident gamma ray and orbital electrons in material. This interaction is the predominant mechanism at intermediate gamma ray energies, ranging from 0.1 to 10 MeV in metals. In Compton scattering, the incoming gamma ray is deflected by a certain angle with respect to its incident direction, and thus imparts a portion of its energy to the electron at rest, which then becomes the recoil electron. The desired displacement cross section for Compton scattering is [42],

$$\sigma_{\gamma}^{\text{CS}}(E_{\gamma}) = \int_0^{E_0^{\text{max}}} \frac{d\sigma^{\text{c}}(E_{\gamma}, E_0)}{dE_0} \cdot \bar{n}(E_0) dE_0 \quad (3-3)$$

Where the kinetic energy of the recoil electron  $E_0$  is a function of scattering angle  $\theta$ ,  $d\sigma^{\text{c}}(E_{\gamma}, E_0)/dE_0$  is the differential scattering cross-section, given by the Klein-Nishina formula. The relationship between the energy of the incident gamma ray and that of the recoil electron is expressed in terms of scattering angle  $\theta$  as:

$$E_0 = \frac{E_{\gamma}(1 - \cos\theta)}{(E_e/E_{\gamma}) + (1 - \cos\theta)} \quad (3-4)$$

Where  $E_e$  is the electron rest mass energy ( $=0.511$  MeV) [28].

### ***3.4.3. Pair production displacement cross-section***

In the process of pair production, the gamma ray is completely absorbed in the field of the nucleus, and an electron-positron pair is created. Pair production is energetically possible only if the gamma ray energy exceeds 1.02 MeV, which corresponds to twice the rest mass energy of an electron. Any excess energy carried by the gamma ray is assumed to be completely converted to kinetic energy shared by the positron and electron. Because the positron subsequently annihilates by combining with an electron, its effect on atomic displacement is not included in the calculation.

Similarly to the photoelectric effect, the pair production displacement cross-section is given by [19],

$$\sigma_{\gamma}^{\text{PP}}(E_{\gamma}) = \sigma^{\text{PP}}(E_{\gamma}, E_0) \cdot \bar{n}(E_0) \quad (3-5)$$

Where;

$$\sigma^{\text{PP}}(E_{\gamma}, E_0) = \sigma_{\text{co}} \cdot Z^2 \left\{ \frac{28}{9} \ln \left( \frac{2E_{\gamma}}{E_e} \right) - \frac{218}{27} \right\} \quad (3-6)$$

### 3.5. Radiation Damage in Solar Cells

The permanent damage in solar cell materials is caused by the collisions of incident radiation particles with atoms in the crystalline lattice, which are displaced from their positions. These defects degrade the transport properties of the material and particularly the minority carrier lifetime. The interaction between vacancies, self-interstitials, impurities, and dopants in Si leads to the formation of undesirable point defects such as recombination and compensator centers which affect performance of solar cells, especially in space.

The introduction of radiation-induced recombination centers reduces the minority carrier lifetime in the base layer of the p-n junction increasing series resistance [43]. Radosavljević and Vasić [31] show that the generation of electron-hole pairs due to ionization effects usually results in the generation and increase of noise and the minimum signal that can be detected. All of these effects lead to the decrease of the output current.

# Chapter Four

## Experimental Measurements

### 4.1. Introduction

The measurements carried out in this experimental work explore the effects of  $^{60}\text{Co}$  and  $^{137}\text{Cs}$   $\gamma$ -photons irradiation on the Photovoltaic parameters of mono-crystalline silicon solar cells.

A suitable (light source - solar cell) geometry was instrumented individually for each  $\gamma$  ray source. each geometry consists of a halogen lamp of 500W power and 100mW.cm<sup>-2</sup> light intensity, and a mono-crystalline silicon solar cell with an active area of 10cm×5cm. At room temperature, the forward bias (I-V) and (P-V) characteristics were determined under illumination, before and after  $\gamma$ -irradiation.

The first solar cell was irradiated with different  $^{60}\text{Co}$   $\gamma$ -exposure doses; 532mR, 1064mR and 1596mR, for 1 hr, 2 hrs and 3 hrs respectively. The second solar cell was irradiated with different  $^{137}\text{Cs}$   $\gamma$ -exposure doses; 280mR, 560mR and 837mR, for 1 hr, 2 hrs and 3 hrs respectively. The results demonstrated that  $\gamma$ -exposure doses have a significant effect on the photovoltaic parameters and it controls the quality and performance of the solar cell. The open circuit voltage ( $V_{oc}$ ), short circuit current ( $I_{sc}$ ), maximum output power ( $P_m$ ) are found to be decreased with  $^{60}\text{Co}$  and  $^{137}\text{Cs}$  gamma exposure doses.

Furthermore the fill factor (FF) and efficiency ( $\eta$ ) are found to be decreased with both  $^{60}\text{Co}$  and  $^{137}\text{Cs}$  gamma exposure doses.

## 4.2. Gamma ray displacement damage

The passage of gamma rays through matter produces electrons and secondary photons in the material. Most of the electrons are produced as the result of the Compton Effect [23]. Pair production and the photoelectric effect are negligible in the range of photon energies with which we are concerned; 1.25 MeV for  $^{60}\text{Co}$  and 0.662 MeV for  $^{137}\text{Cs}$  [35].

These  $\gamma$ -induced electrons have a spectrum of energies ranging upward to 0.8 MeV [44]. In addition, transfer energy to a lattice atom through an electron-atom scattering event. Atoms are bound to lattice sites and a certain amount of energy must be imparted to the atom in order to displace it from its normal site and create a vacancy-interstitial pair. In silicon, this minimum energy  $E_d$  is about 13eV [24]. The energy  $E_t$  which an electron must have in order to impart energy  $E_d$  to the struck atom is related to  $E_d$  by the following [45]:

$$E_d = \frac{2m_e}{M_2} \frac{E_t}{m_e c^2} (E_t + 2m_e c^2) \quad (4-1)$$

For silicon,  $E_t$ , is about 0.14MeV.

### **4.3. Effect of displaced atoms on solar cell performance**

The permanent damage in the solar cells materials is caused by collisions of the incident radiation particles with the atoms in the crystalline lattice, which are displaced from their positions. These defects degrade the transport properties of the material and particularly the minority carrier lifetime [46-48]. Photovoltaic parameters of silicon solar cell such open circuit voltage ( $V_{oc}$ ), short circuit current ( $I_{sc}$ ), maximum output power ( $P_m$ ), fill factor (FF) and efficiency ( $\eta$ ), strongly depend on minority carrier life time [49]. And several authors [48, 50] have reported that a decrease in the minority carrier life time reduce the electric properties of solar cells. This work examine a suitable (light source-solar cell) geometry and describes a series of measurements carried out to characterize the  $^{60}\text{Co}$  and  $^{137}\text{Cs}$   $\gamma$ -induced displacement damage on a mc-Si solar cell in terms of variation of mc-Si solar cell photovoltaic parameters with respect to  $^{60}\text{Co}$  and  $^{137}\text{Cs}$   $\gamma$ -ray exposure doses.

### **4.4. Instrumentation**

Schematic diagram for the circuit considered for measuring the photovoltaic output parameters of the solar cell under test is shown in Fig.4-1. A photograph for the light source-solar cell geometry is shown in Fig.4-2.



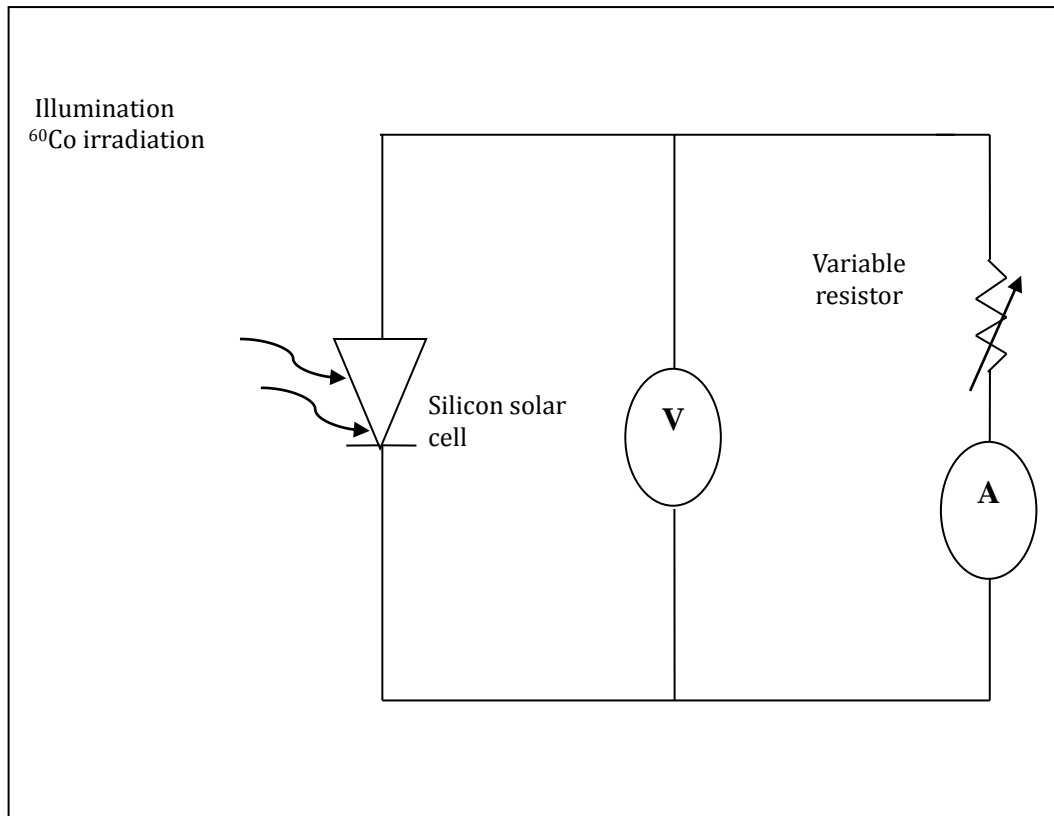


**Fig. 4-1: Schematic diagram for the circuit utilized for measurements**

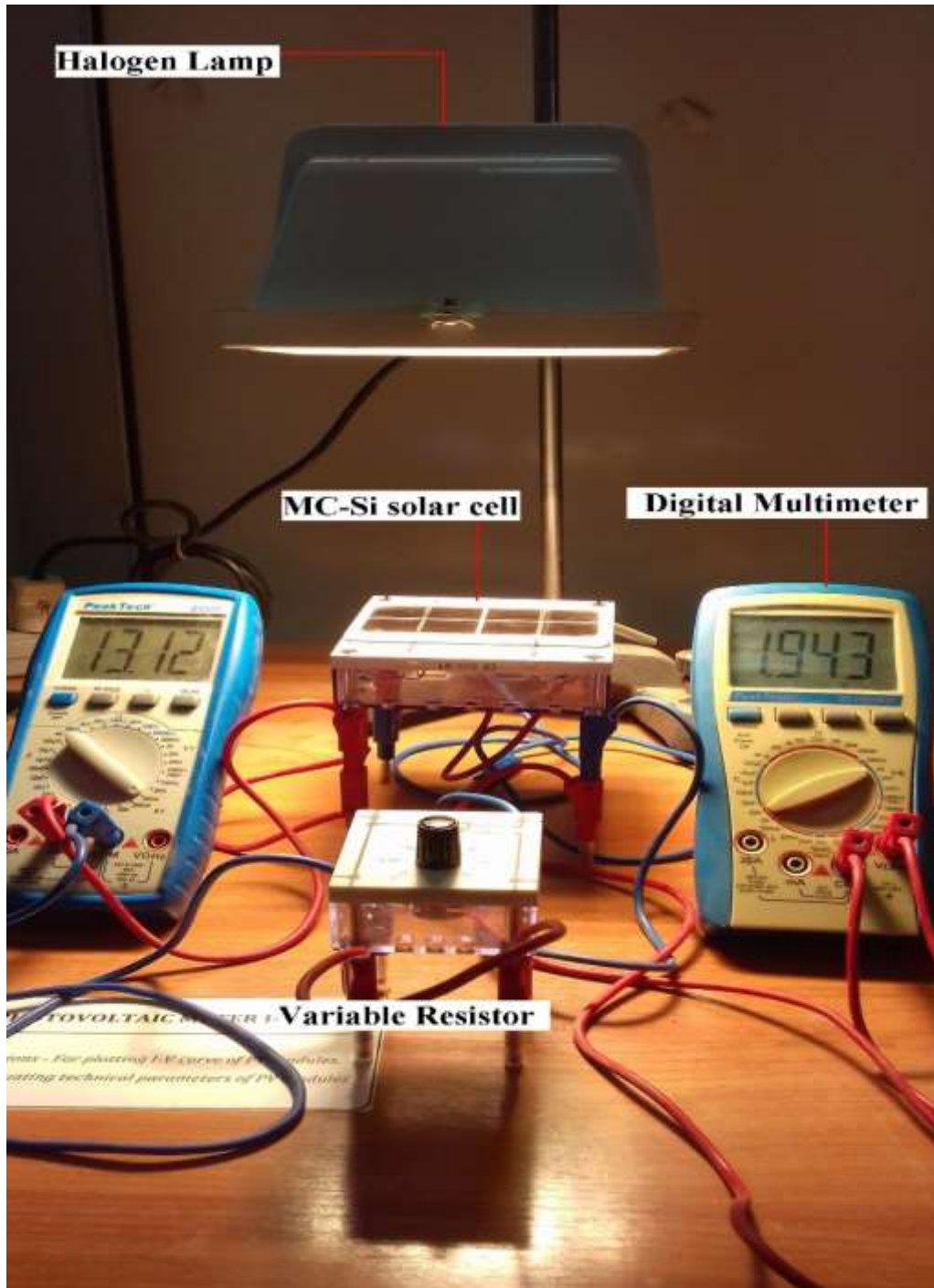


**Fig.4-2: A photograph for the (light source-solar cell) geometry**

The solar cell under test was a commercial mc-Si solar cell with an active area of 10cm×5cm manufactured by Leybold [51].

The employed light source was a 500 W halogen lamp. In a Cartesian system of reference where the y-axis coincides with the solar cell axis and is directed upwards, the light source was fixed at y=20 cm above the active surface area of the solar cell. This will provide a 90<sup>0</sup> incident angle for photons of the light source. The halogen lamp bulb is inexpensive, uncomplicated and convenient to operate and require only easy power supply units. The halogen lamp bulb is widely used in solar beam experiments (SBE) for solar simulator applications because it provides a very stable and smooth spectral output [52]. The light source intensity was measured to be 100 mW.cm<sup>-2</sup>. This value simulates AM1.5 solar radiation over the active area of the solar cell [53]. The light intensity was measured using a pyranometer type HT303N of sensitivity 19.8μV/W.m<sup>-2</sup>, connected to a solar systems analyzer type HTSolar300.

First for γ-ray irradiation, a <sup>60</sup>Co γ-ray source of activity 1mCi and average energy of 1.25meV was utilized. Two digital multimeters were used to record the output voltage and current while varying the value of a variable resistor (0-1KΩ).

After gathering the results of the <sup>60</sup>Co γ-ray exposure, the <sup>60</sup>Co γ-ray source was replaced with a <sup>137</sup>Cs γ-ray source and a new mono-crystalline silicon solar cell with an active area of 10cm×5cm was instrumented and the output voltage and current were recorded using Two digital multimeters while varying the value of a variable resistor (0-1KΩ). Fig.4-3 shows a photograph for the light

source-solar cell geometry during gamma exposure. Fig.4-4 shows the solar systems analyzer type HTSolar300 used to measure The light intensity , Fig.4-5 shows the pyranometer type HT303N of sensitivity  $19.8\mu\text{V}/\text{W}\cdot\text{m}^{-2}$  also used to measure the light intensity .

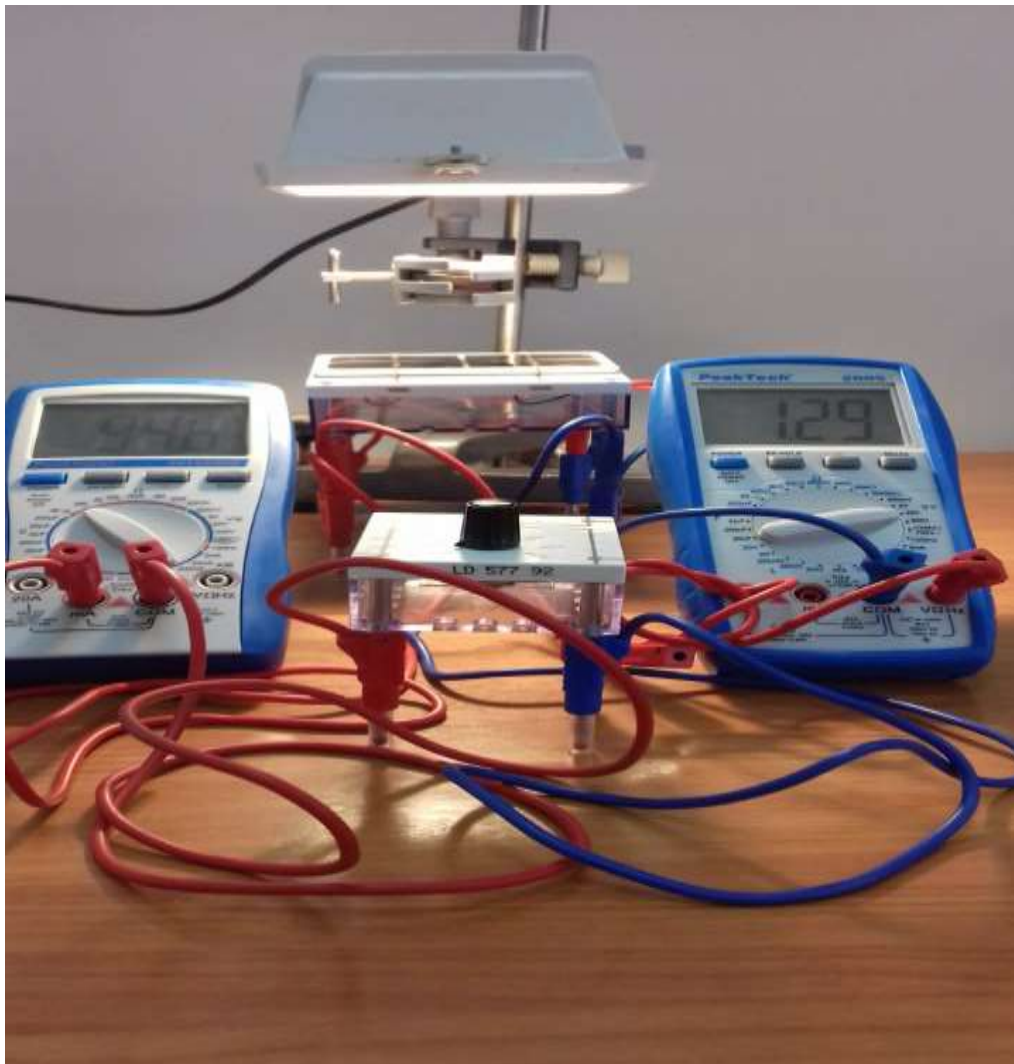


**Fig (4-3) A photograph for the (light source-solar cell) geometry during gamma exposure**



**Fig (4-4) A solar analyzer type HTSolar300 used to measure the light intensity**



**Fig (4-5) A pyranometer type HT303N of sensitivity  $19.8\mu\text{V}/\text{W}\cdot\text{m}^{-2}$  used to measure the light intensity**

## 4.5. Measurements Procedure

The forward bias I-V characteristics of mc-Si solar cells, before and after gamma ray irradiation, were measured at room temperature for different periods of time. The light source was used to uniformly illuminate the solar cell under test and the measurements were performed within 15 minutes in room temperature. It is important to carry out the measurements within a short time scale ( $\sim 0.25$  % hour) to avoid elevating the cell temperature, as this will result in a decrease of  $V_{oc}$ , with a relative reduction in light conversion efficiency of about  $0.4\% K^{-1}$  [54]. The variable resistor, R was set to its maximum value ( $1K\Omega$ ) and both the current (I) and the voltage (V) were recorded. At  $R=1K\Omega$ , within our measurement conditions, the voltage will approximate the open-circuit value  $V_{oc}$ . The resistance was then decreased in steps. Both I and V were recorded for different settings, including the short-circuit current  $I_{sc}$  corresponding to  $R=0$ . At this point, the light source was turned off and the  $^{60}Co$   $\gamma$ -source was located at the  $y=5cm$  above the active area of the Si solar cell. The cell was irradiated for 1 hr, 2hrs and 3 hrs. The corresponding exposures were calculated to be 532 mR, 1064 mR and 1596 mR, respectively. At the end of each exposure time, the  $^{60}Co$   $\gamma$ - source is removed and the light source is turned on. The data for I and V including  $I_{sc}$  and  $V_{oc}$  were recorded following the measurements procedure before  $^{60}Co$   $\gamma$ -ray irradiation.



The I-V characteristics, before and after  $^{60}\text{Co}$   $\gamma$ -irradiation were used to determine the point of maximum power ( $V_{mp}$ ,  $I_{mp}$ ) and calculate the fill factor FF. At this point, the output power values including the maximum output values ( $P_{mp}$ ,  $V_{oc}$ ,  $I_{sc}$ , FF) were calculated and (P-V) characteristics were generated.

On the basis of the I-V characteristics, Solar cell parameters like short circuit current ( $I_{sc}$ ), open circuit voltage ( $V_{oc}$ ), fill factor (ff) and efficiency ( $\eta$ ) can be calculated. The fill factor (FF) is a key performance parameter for solar cells and can be expressed as;

$$FF = \frac{V_{mp} I_{mp}}{V_{oc} I_{sc}} \quad (4-2)$$

Where  $V_{mp}$  and  $I_{mp}$  are the voltage and the current at a maximum power point, and  $V_{oc}$  and  $I_{sc}$  are the open circuit voltage and short circuit current respectively [55]. The efficiency ( $\eta$ ) for a solar cell is given by;

$$\eta = \frac{V_{oc} I_{sc} FF}{P_{in}} \quad (4-3)$$

Where  $I_{sc}$  is the short circuit current,  $V_{oc}$  is the open circuit voltage and  $P_{in}$  is the incident light power.

A new (light source- solar cell) geometry was instrumented and all the steps mentioned above was repeated using a  $^{137}\text{Cs}$   $\gamma$ -source for irradiation. The gamma source was located at  $y=5\text{cm}$  above the active area of the Si solar cell. The cell was irradiated for 1hr, 2hrs and 3hrs. The corresponding exposures were calculated to be 280 mR, 560 mR and 837 mR, respectively.

## Chapter Five

### Results discussion and conclusion

#### 5.1. Introduction

This work characterizes the  $^{60}\text{Co}$  and  $^{137}\text{Cs}$   $\gamma$ -induced displacement damage on mc-Si solar cells in terms of variation of photovoltaic parameters. The forward bias (I-V) characteristics and the rest of measurements were carried out at room temperature.

#### 5.2. Effects of illumination of $^{60}\text{Co}$ $\gamma$ -ray irradiation on the I-V and P-V characteristics

The forward bias I-V characteristics of the mc-Si solar cell, before and after various  $^{60}\text{Co}$   $\gamma$ -ray exposure doses; 532 mR, 1064 mR and 1596 mR, were measured at room temperature and shown in table (5.1) and Fig.(5.1). In comparison to the voltage  $V_{\text{mp}}$  and current  $I_{\text{mp}}$  values before  $^{60}\text{Co}$   $\gamma$ -ray irradiations, the  $V_{\text{mp}}$  values after irradiation were deteriorated by approximately 0.4% ,2.9% ,9%, respectively , while the  $I_{\text{mp}}$  values after irradiation were deteriorated by 9.7%, 12% and 17.5%, respectively. The variation of the output power with voltage; (P-V) characteristics are reported in table (5.1) and Fig (5.2). As shown, in comparison to the output power values before  $^{60}\text{Co}$   $\gamma$ -ray exposure doses, the  $P_{\text{mp}}$  values after irradiation were deteriorated by approximately 10%, 14.5% and 24.9%, respectively.

The results reported in Fig.(5.1) and Fig.(5.2) in one hand, re-confirm the deterioration of the I-V and P-V characteristics of the solar cell due to increasing of gamma exposure values and on the other hand demonstrate the feasibility of our proposed (light source-solar cell) geometry.

**Table (5.1):The illuminated I-V ; P-V characteristics of mc-Si solar cell irradiated with 1.25 MeV  $^{60}\text{Co}$  photons at various doses collectively.**

Condition	Parameters		
Pre irradiation	$I_{mp}$	$V_{mp}$	$P_{mp}$
	0.937753	0.5401944	0.506569
After irradiation	$I_{mp}$	$V_{mp}$	$P_{mp}$
$^{60}\text{Co}$ (Dose 1) 532 mR	0.846737	0.53784823	0.455416
$^{60}\text{Co}$ (Dose 2) 1064 mR	0.825667	0.52443782	0.433011
$^{60}\text{Co}$ (Dose 3) 1596 mR	0.773946	0.49154851	0.380432

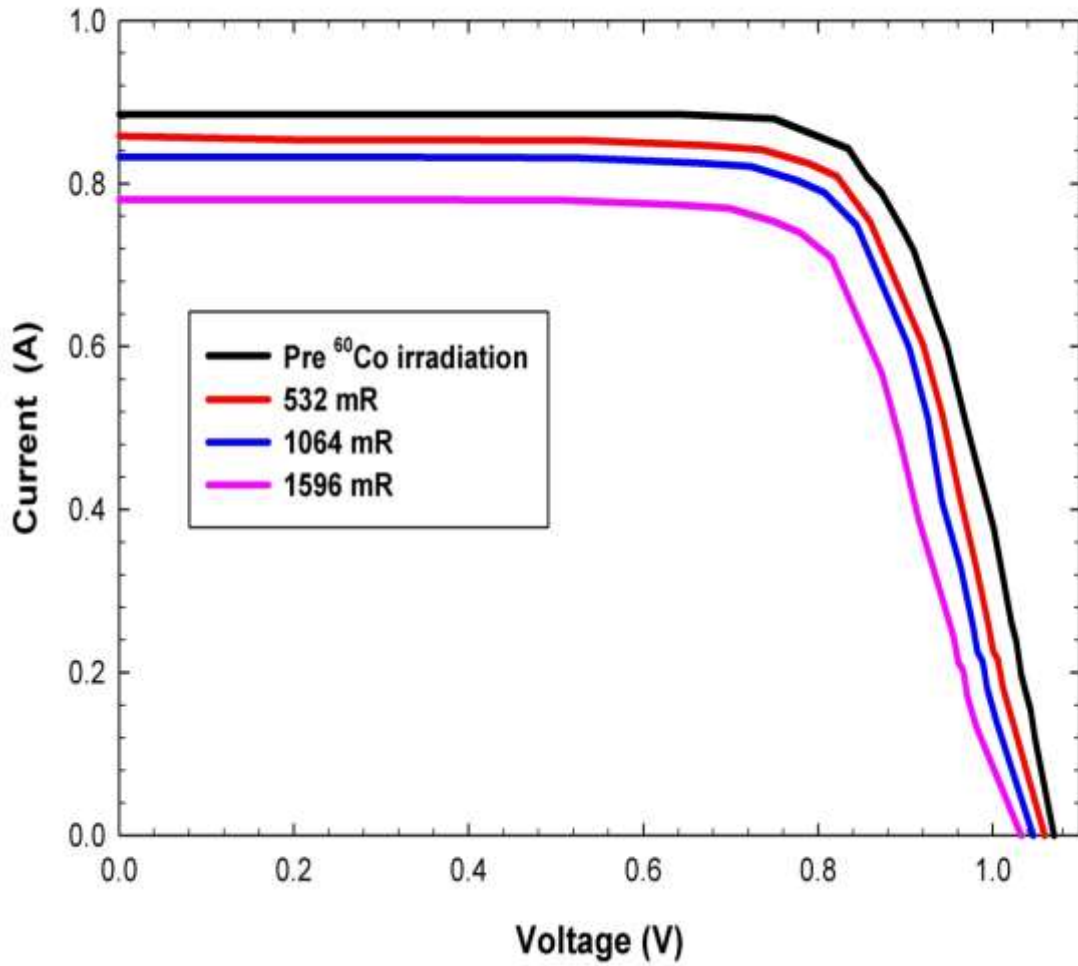


**Fig. (5.1) The illuminated I-V characteristics of mc-Si solar cell irradiated with 1.25 MeV <sup>60</sup>Co photons at various doses collectively.**

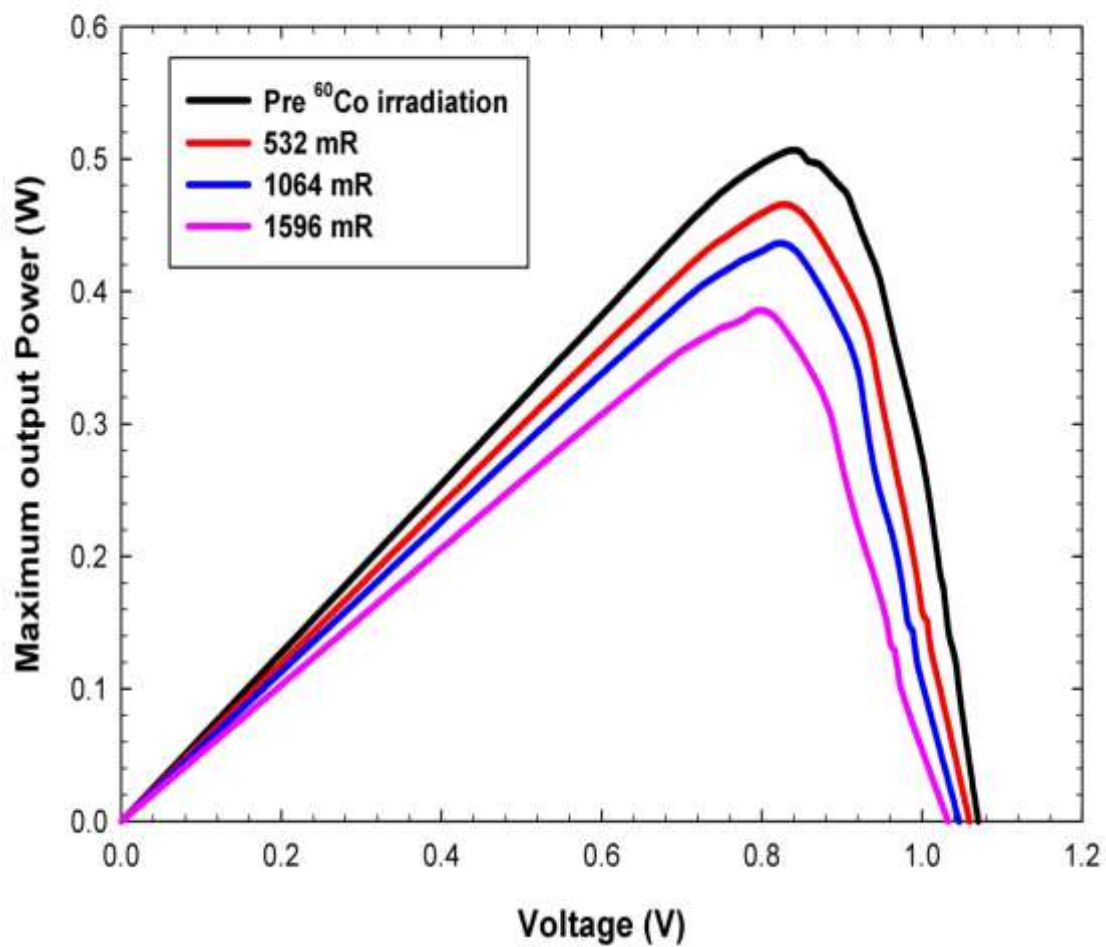


**Fig. (5.2):** The illuminated P-V characteristics of mc-Si solar cell irradiated with 1.25 MeV <sup>60</sup>Co photons at various doses collectively.

### 5.3. Effects of illumination of $^{60}\text{Co}$ $\gamma$ -ray irradiation on $V_{oc}$ , $I_{sc}$ , FF and $\eta$

The variations of mc-Si solar cell photovoltaic parameters; open circuit voltage ( $V_{oc}$ ) and short circuit current ( $I_{sc}$ ) with respect to gamma exposure doses are reported in table (5.2) and shown in Fig (5.3). While those for fill factor (FF) and efficiency ( $\eta$ ) are also reported in table (5.2) and shown in Fig(5.4). All parameters under investigation were normalized to the values obtained before  $^{60}\text{Co}$   $\gamma$ -ray irradiations. It was found that the degradation of mc-Si solar cell photovoltaic parameters is dependent on the gamma exposure doses; 532 mR, 1064 mR and 1596 mR. As shown in Fig.(5.3), The  $V_{oc}$  and  $I_{sc}$  values were deteriorated by approximately 1.5 %, 2.2% and 3% for  $V_{oc}$ , and 3%, 6% and 11.9% for  $I_{sc}$ , respectively.

As reported in Fig.(5.4), the FF values were deteriorated by approximately 5.9%, 7.1% and 12.2% respectively. while the  $\eta$  values deteriorated by 9% for exposure dose 532mR, 13.4% for exposure dose 1064mR and 24% for exposure dose 1596mR . The results re-confirm the deterioration effect of  $^{60}\text{Co}$   $\gamma$ -induced displacement damage on the photovoltaic parameters of the mc-Si solar cells.



**Table (5.2): Variation of normalized  $V_{oc}$   $I_{sc}$  FF and  $\eta$  with  $^{60}\text{Co}$   
 $\gamma$ - exposure doses**

Condition	Parameters			
Pre irradiation	$V_{oc}$	$I_{sc}$	FF	$\eta$
	1.0000	1.0000	0.506569	0.001
After irradiation	$V_{oc}$	$I_{sc}$	FF	$\eta$
$^{60}\text{Co}$ (Dose 1) 532 mR	0.9850	0.9701	0.476601	0.000910
$^{60}\text{Co}$ (Dose 2) 1064 mR	0.9783	0.9405	0.470617	0.000866
$^{60}\text{Co}$ (Dose 3) 1596 mR	0.9701	0.8815	0.444875	0.000760

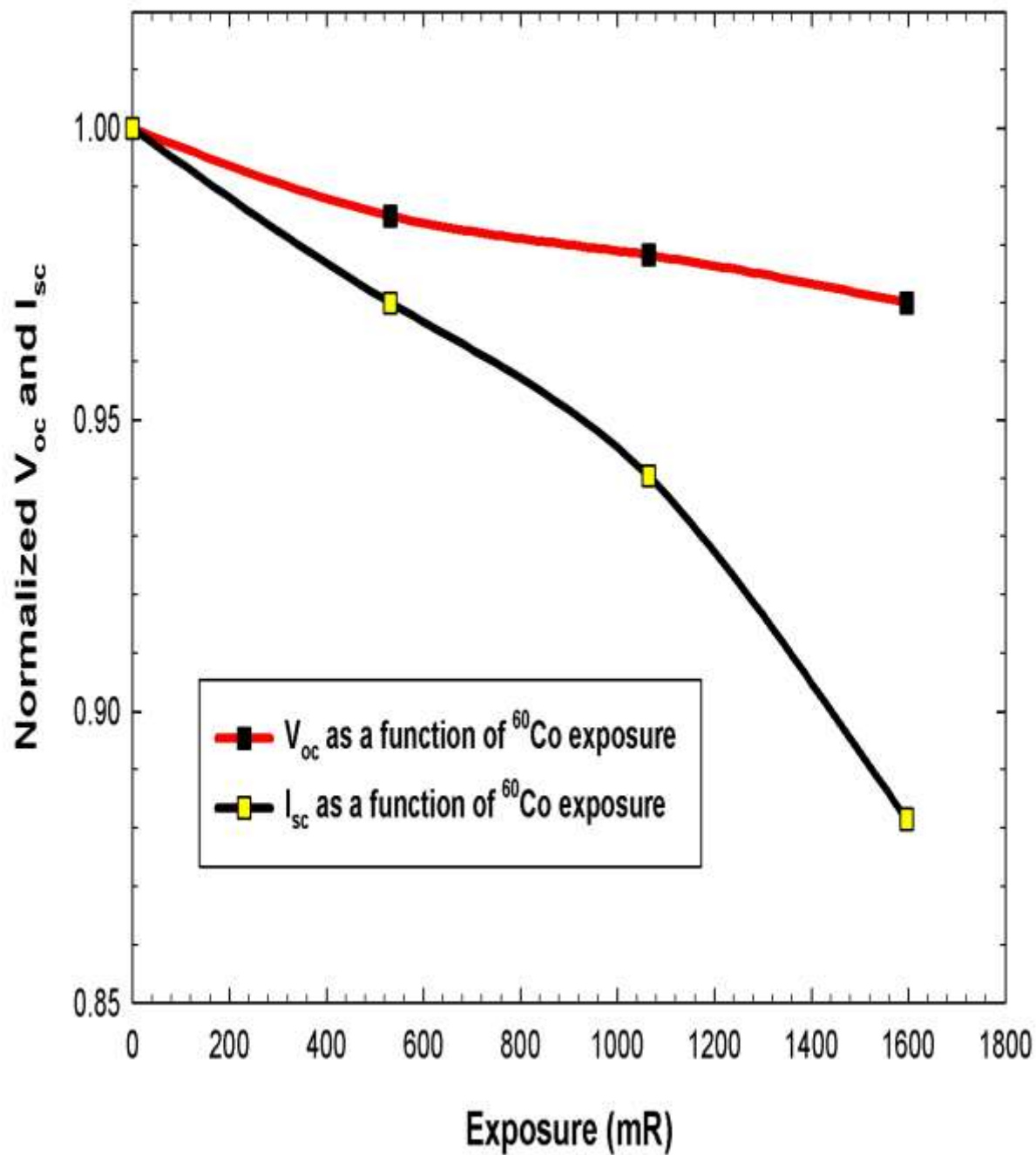


**Fig. (5.3): Variation of normalized  $V_{oc}$  and  $I_{sc}$  with  $^{60}\text{Co}$   $\gamma$ - exposure doses**

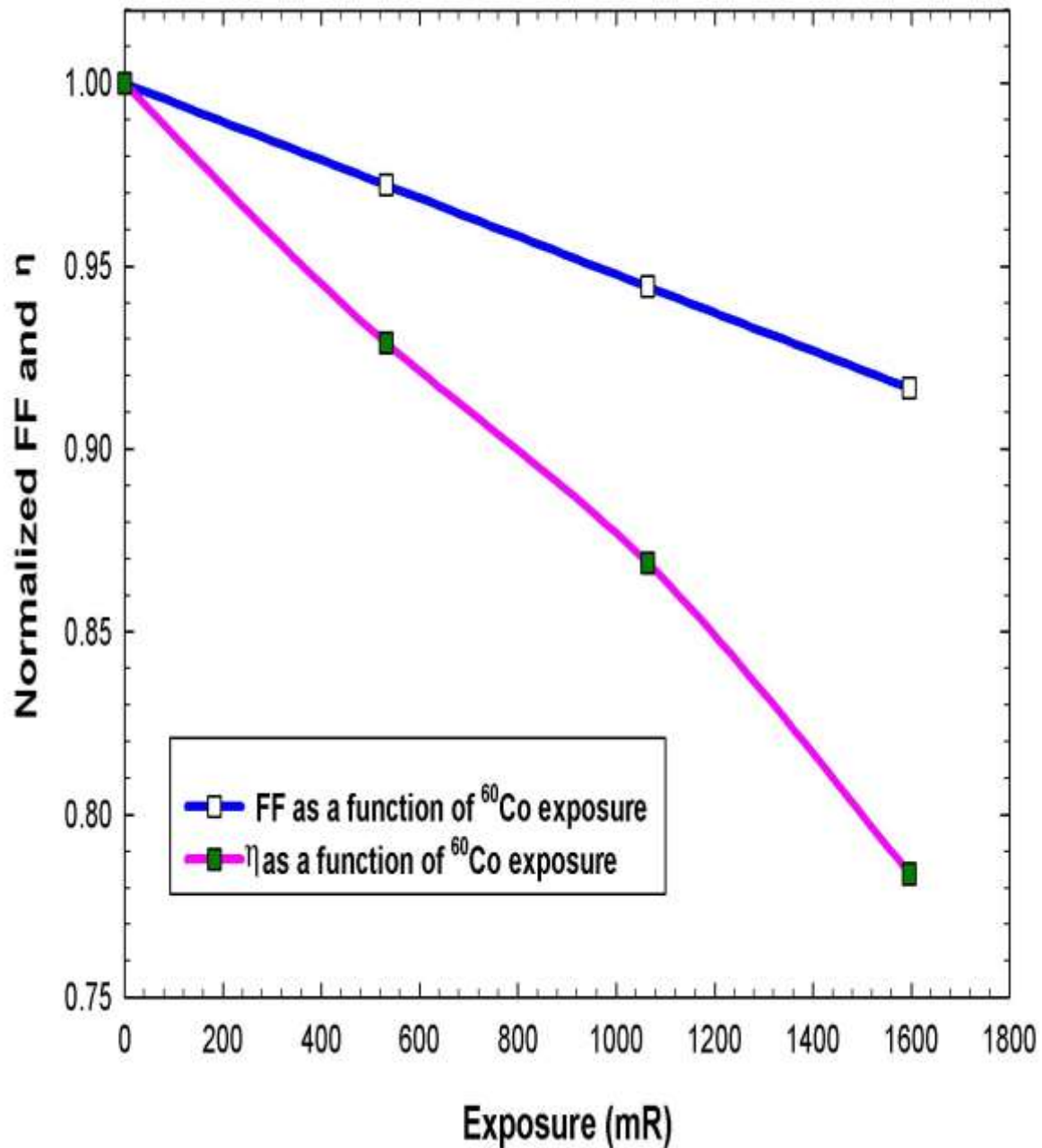


**Fig. (5.4): Variation of normalized FF and  $\eta$  with  $^{60}\text{Co}$   $\gamma$ - exposure doses**

**5.4. Effects of illumination of  $^{137}\text{Cs}$   $\gamma$ -ray irradiation on the I-V and P-V**

## characteristics

The forward bias I-V characteristics of the mc-Si solar cell, before and after various  $^{137}\text{Cs}$   $\gamma$ -ray exposure doses; 280 mR, 560 mR and 837 mR, were measured at room temperature at different periods of time and shown table (5.3) and in Fig. (5.5). In comparison to the voltage  $V_{\text{mp}}$  and current  $I_{\text{mp}}$  values before  $^{137}\text{Cs}$   $\gamma$ -ray irradiations, the  $V_{\text{mp}}$  values after irradiation were deteriorated by approximately 0.4% ,2.9% ,9%, respectively, while the  $I_{\text{mp}}$  values were deteriorated by 7.9%, 10.1% and 13.3%, respectively. The variation of the output power with voltage; (P-V) characteristics are reported table (5.3) and in Fig (5.6). As shown, in comparison to the output power values before  $^{137}\text{Cs}$   $\gamma$ -ray exposure doses, the  $P_{\text{mp}}$  values after irradiation were deteriorated by approximately 8.3%, 12.8% and 21.1%, respectively.

The results reported in Fig (5.5) and Fig (5.6) in one hand, re-confirm the deterioration of the I-V and P-V characteristics of the solar cell due to increasing of gamma exposure values and on the other hand demonstrate the feasibility of our proposed (light source-solar cell) geometry.

**Table (5.3):The illuminated I-V ; P-V characteristics of mc-Si solar cell irradiated with 0.662 MeV <sup>137</sup>Cs photons at various doses collectively.**

condition	Parameters		
Pre irradiation	I <sub>mp</sub>	V <sub>mp</sub>	P <sub>mp</sub>
	0.937753	0.5401944	0.506569
After irradiation	I <sub>mp</sub>	V <sub>mp</sub>	P <sub>mp</sub>
<sup>137</sup> Cs (Dose 1) 280 mR	0.863672	0.53807927	0.464724
<sup>137</sup> Cs (Dose 2) 560 mR	0.842181	0.52443833	0.441672
<sup>137</sup> Cs (Dose 3) 837 mR	0.812643	0.49155533	0.399459

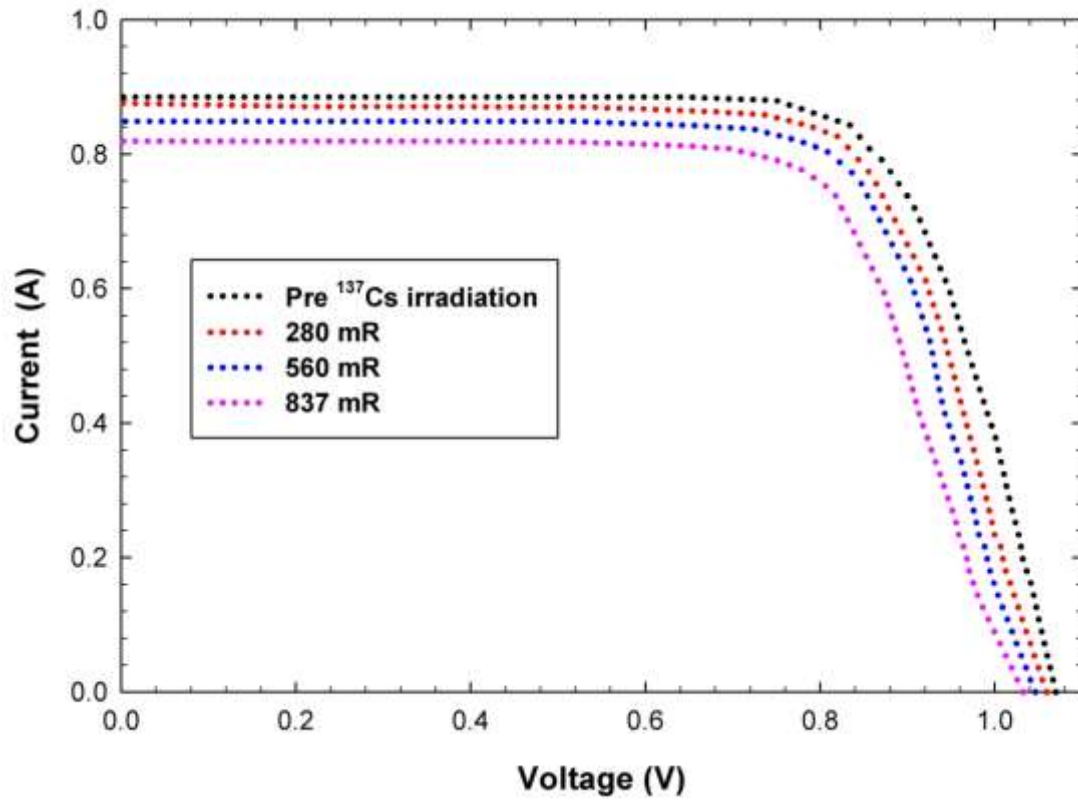


**Fig (5.5): The illuminated I-V characteristics of mc-Si solar cell irradiated with 0.662 MeV photons at various doses collectively.**

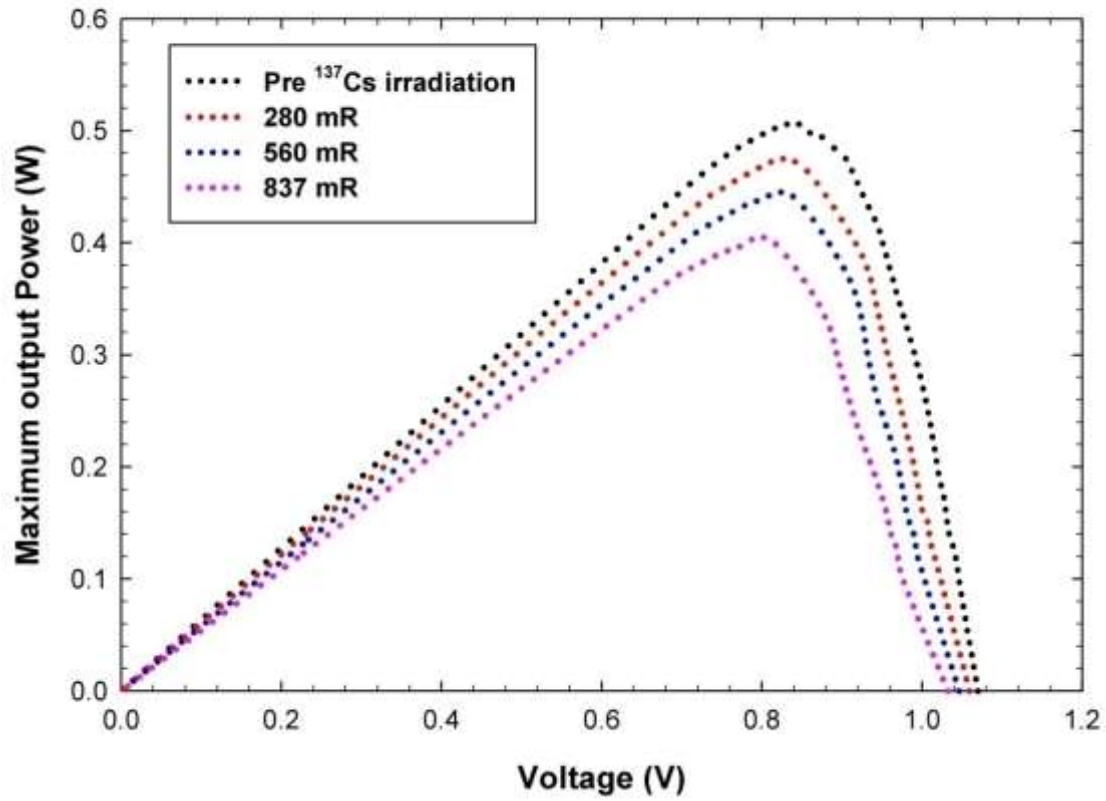


**Fig. (5.6):** The illuminated P-V characteristics of mc-Si solar cell irradiated with 0.662 MeV photons at various doses collectively.

## 5.5. Effects of illumination of $^{137}\text{Cs}$ $\gamma$ -ray irradiation on $V_{oc}$ , $I_{sc}$ , FF and $\eta$

The variations of mc-Si solar cell photovoltaic parameters; open circuit voltage ( $V_{oc}$ ) and short circuit current ( $I_{sc}$ ) with respect to gamma exposure doses are reported in table (5.4), beside those for fill factor (FF) and efficiency ( $\eta$ ). All parameters under investigation were normalized to the values obtained before  $^{137}\text{Cs}$   $\gamma$ -ray irradiations. It was found that the degradation of mc-Si solar cell photovoltaic parameters is dependent on the gamma exposure doses; 280 mR, 560 mR and 837 mR. As shown in table.(5.4), The  $V_{oc}$  and  $I_{sc}$  values were deteriorated by approximately 0.9%, 1.6% and 2% for  $V_{oc}$ , and 2%, 5% and 10.9% for  $I_{sc}$ , respectively.

As reported in table (5.4), the FF values were deteriorated by approximately 5.5%, 6.8% and 9.7% respectively. while the  $\eta$  values deteriorated by 7.1% for exposure dose 280mR, 11.7% for exposure dose 560mR and 20.2% for exposure dose 837mR. The results re-confirm the deterioration effect of  $^{137}\text{Cs}$   $\gamma$ -induced displacement damage on the photovoltaic parameters of the mc-Si solar cells.



**Table (5.2): Variation of normalized  $V_{oc}$   $I_{sc}$  FF and  $\eta$  with  $^{137}\text{Cs}$   $\gamma$ - exposure doses**

Condition	Parameters			
Pre irradiation	$V_{oc}$	$I_{sc}$	FF	$\eta$
	1.0000	1.0000	0.506569	0.001
After irradiation	$V_{oc}$	$I_{sc}$	FF	$\eta$
$^{137}\text{Cs}$ (Dose 1) 532 mR	0.9910	0.9800	0.478514	0.000929
$^{137}\text{Cs}$ (Dose 2) 1064 mR	0.9843	0.9502	0.472234	0.000883
$^{137}\text{Cs}$ (Dose 3) 1596 mR	0.9800	0.8912	0.457373	0.000798

## 5.6. Comparison between the Effects of illumination of $^{60}\text{Co}$ and $^{137}\text{Cs}$ $\gamma$ -ray irradiation on the I–V and P-V characteristics

The forward bias I-V characteristics of two mc-Si solar cells, after various  $^{60}\text{Co}$   $\gamma$ -ray exposure doses; 532 mR, 1064 mR and 1596 mR for the first cell, and  $^{137}\text{Cs}$   $\gamma$ -ray exposure doses; 280 mR, 560 mR and 837 mR for the second cell, were measured at room temperature at the same acquisition time 1 hr ,2 hrs ,3hrs for both sources individually, compared and shown in Fig(5.7) (a,b,c,).

As seen in Fig (5.7)(a), the maximum (I-V) point for  $^{137}\text{Cs}$  peaks at (0.863672, 0.53807927) where for  $^{60}\text{Co}$  it peaks at (0.846737, 0.53784823), in Fig (5.7)(b), the maximum (I-V) point for  $^{137}\text{Cs}$  peaks at (0.842181, 0.52443833) where for  $^{60}\text{Co}$  it peaks at (0.825667, 0.52443782), in Fig (5.7)(c), the maximum (I-V) point for  $^{137}\text{Cs}$  peaks at (0.812643, 0.49155533) where for  $^{60}\text{Co}$  it peaks at (0.773946, 0.49154851), In comparison to the voltage  $V_{\text{mp}}$  values after  $^{137}\text{Cs}$   $\gamma$ -ray irradiations the  $V_{\text{mp}}$  values of  $^{137}\text{Cs}$   $\gamma$ -ray irradiations exceeds those of  $^{60}\text{Co}$   $\gamma$ -ray irradiations by 0.04%, 0.0001% and 0.001%, respectively. In comparison to the current  $I_{\text{mp}}$  values after  $^{137}\text{Cs}$   $\gamma$ -ray irradiations the  $I_{\text{mp}}$  values of  $^{137}\text{Cs}$   $\gamma$ -ray irradiations exceed those of  $^{60}\text{Co}$   $\gamma$ -ray irradiations by 1.96%, 2% and 4.9%, respectively.

The variation of the output power with voltage ;( P-V) characteristics are reported in Fig (5.8) (a,b,c,). As shown in Fig (5.8) (a), the maximum (P-V) point for  $^{137}\text{Cs}$  peaks at (0.464724) where for  $^{60}\text{Co}$  it peaks at (0.455416), in Fig (5.8)(b), the maximum (P-V) point for  $^{137}\text{Cs}$  peaks at (0.441672) where for  $^{60}\text{Co}$  it peaks at (0.433011), in Fig (5.8)(c), the maximum (P-V) point for  $^{137}\text{Cs}$  peaks at (0.399459) where for  $^{60}\text{Co}$  it peaks at (0.380432), , in comparison to the output power values after  $^{137}\text{Cs}$   $\gamma$ -ray exposure , the  $P_{\text{mp}}$  values of  $^{137}\text{Cs}$   $\gamma$ -ray irradiations exceeds those of  $^{60}\text{Co}$   $\gamma$ -ray irradiations by 2%, 1.9% and 4.7 %, respectively.

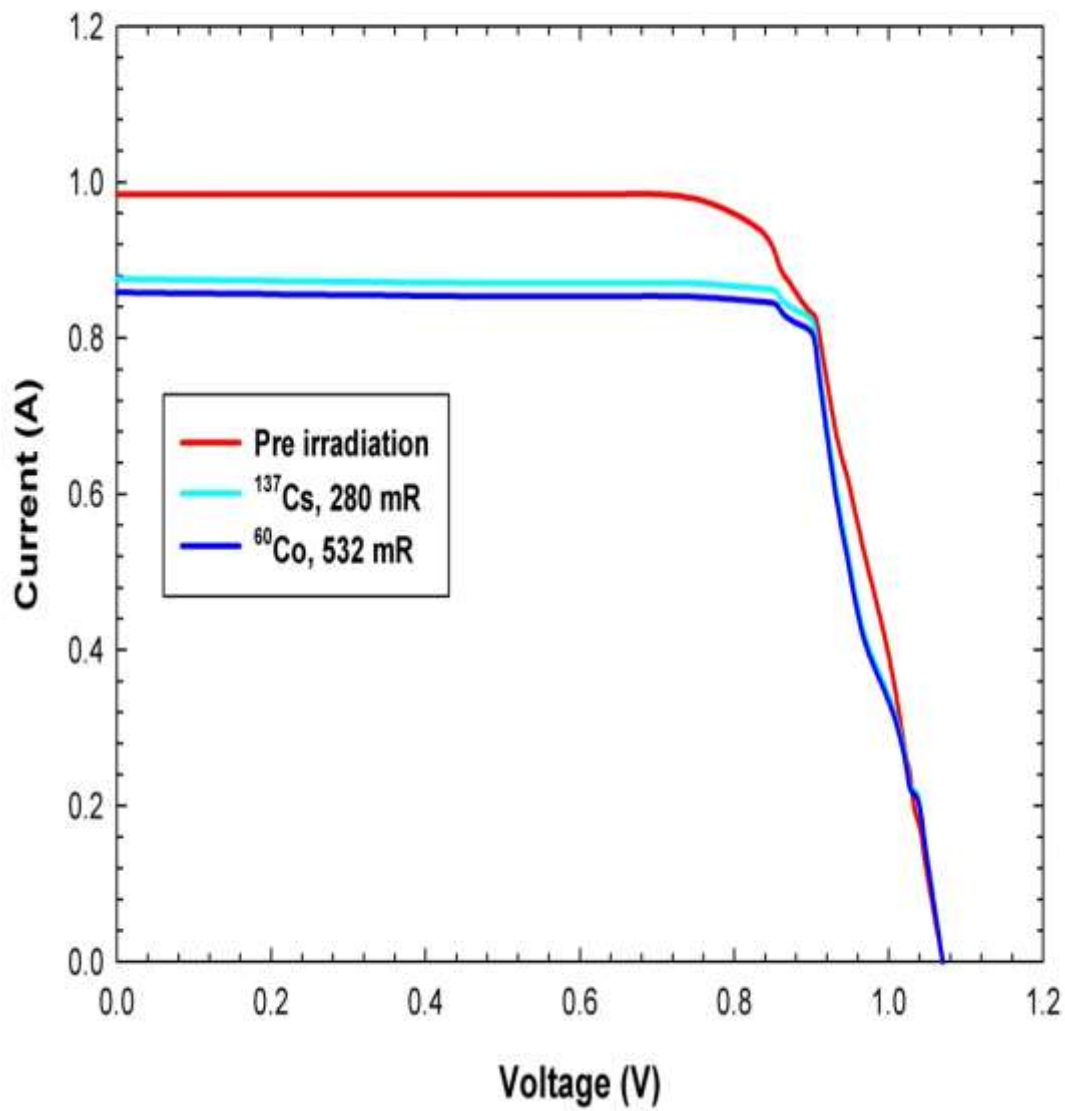


**Fig (5.7.a): The illuminated I-V characteristics of mc-Si solar cell irradiated with 532 mR <sup>60</sup>Co gamma photons VS 280 mR <sup>137</sup>Cs gamma photons.**

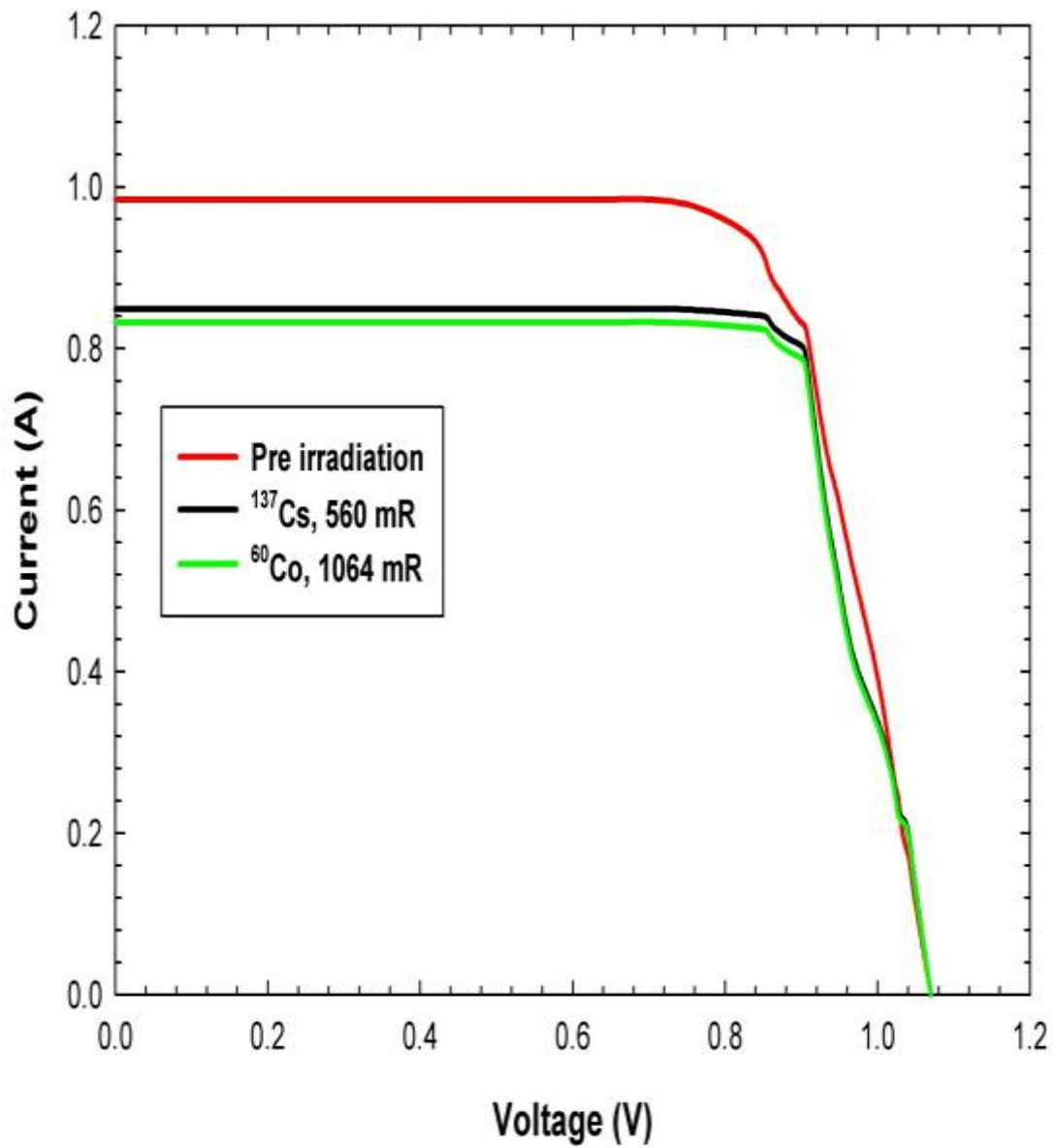


**Fig (5.7.b): The illuminated I-V characteristics of mc-Si solar cell irradiated with 1064 mR <sup>60</sup>Co gamma photons VS 560 mR <sup>137</sup>Cs gamma.**

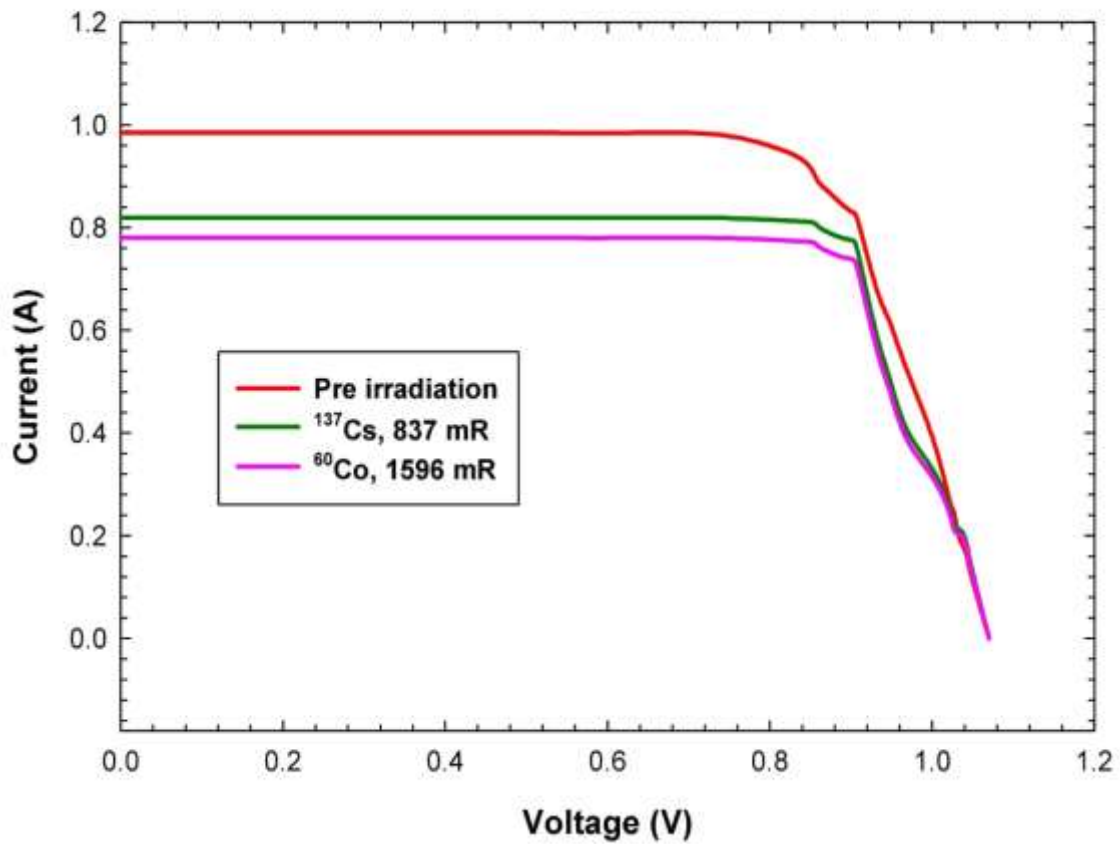


**Fig (5.7.c): The illuminated I-V characteristics of mc-Si solar cell irradiated with 1596 mR <sup>60</sup>Co gamma photons VS 837 mR <sup>137</sup>Cs gamma.**

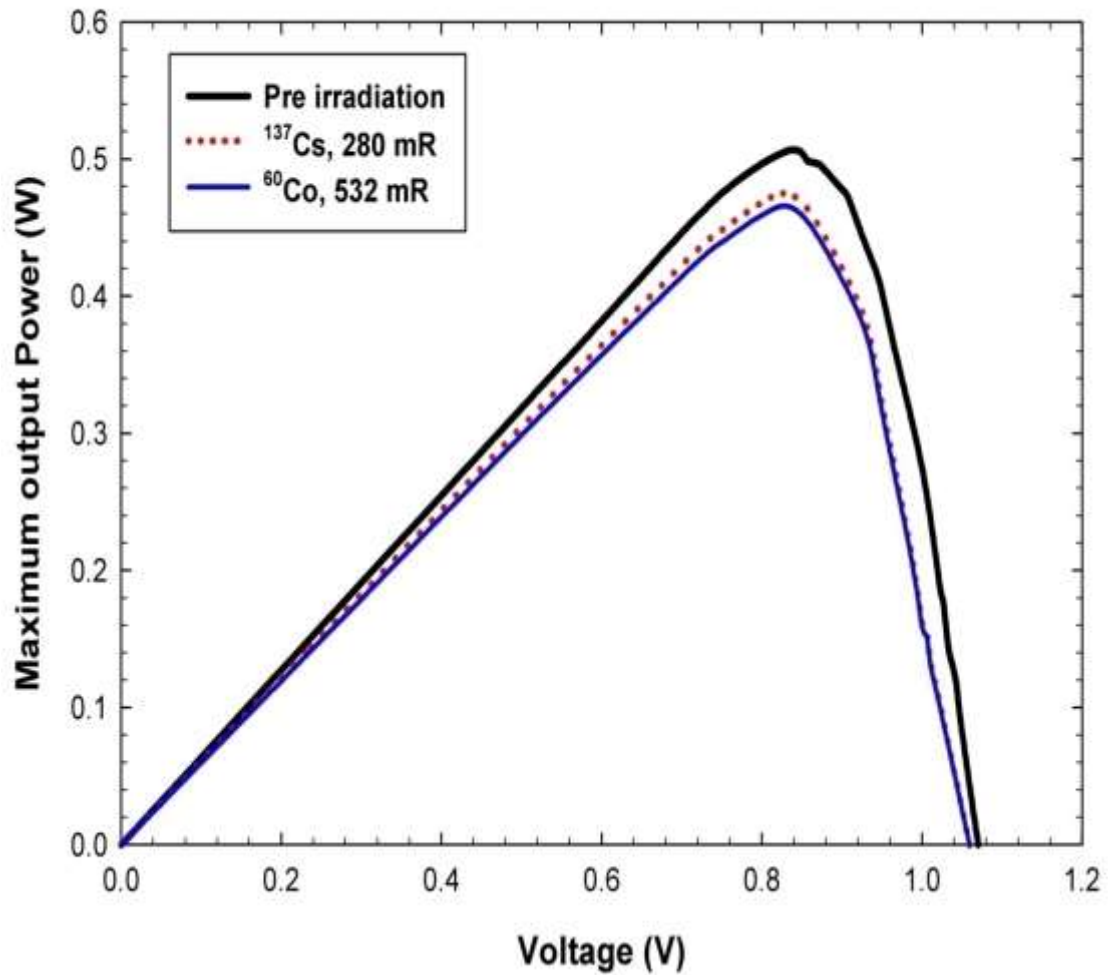


**Fig (5.8.a): The illuminated P-V characteristics of mc-Si solar cell irradiated with 532 mR <sup>60</sup>Co gamma photons VS 280 mR <sup>137</sup>Cs gamma.**

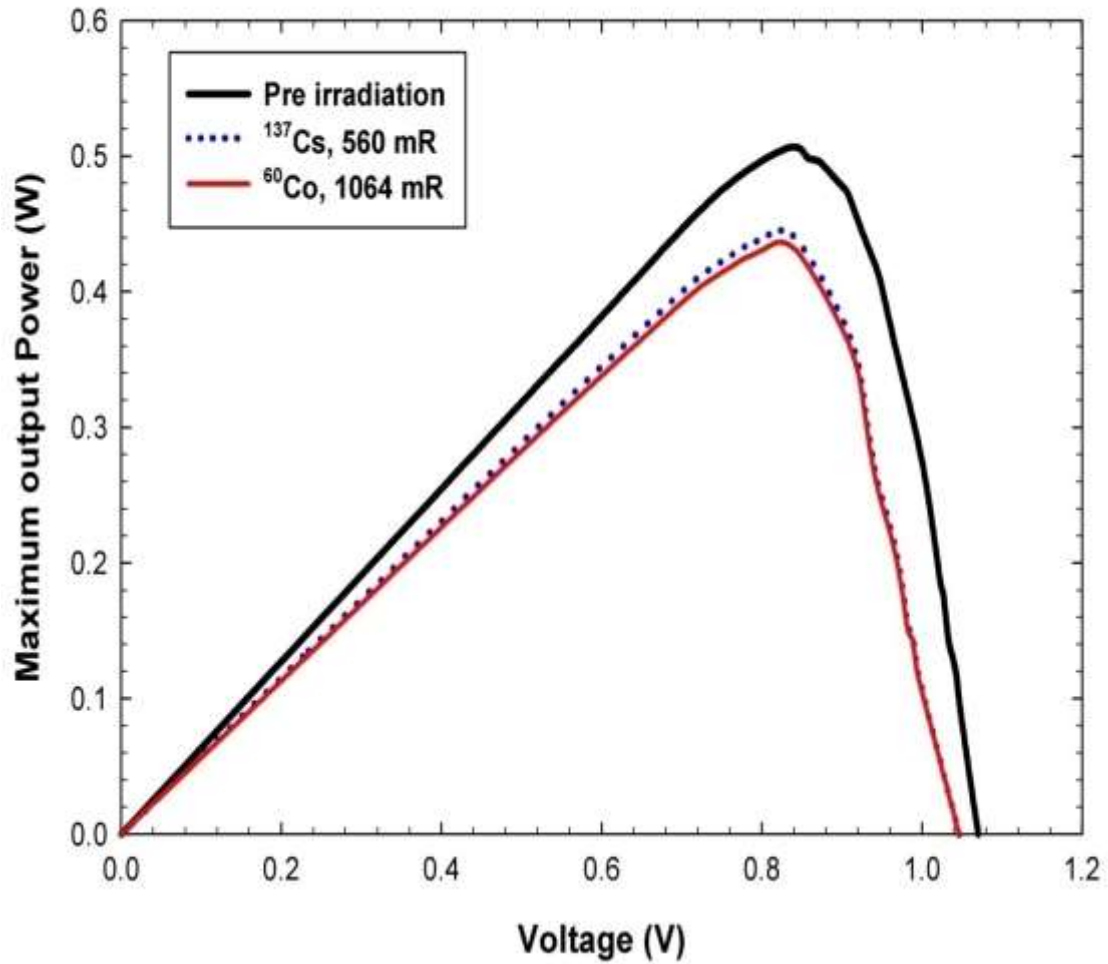


**Fig (5.8.b): The illuminated P-V characteristics of mc-Si solar cell irradiated with 1064 mR <sup>60</sup>Co gamma photons VS 560 mR <sup>137</sup>Cs gamma.**



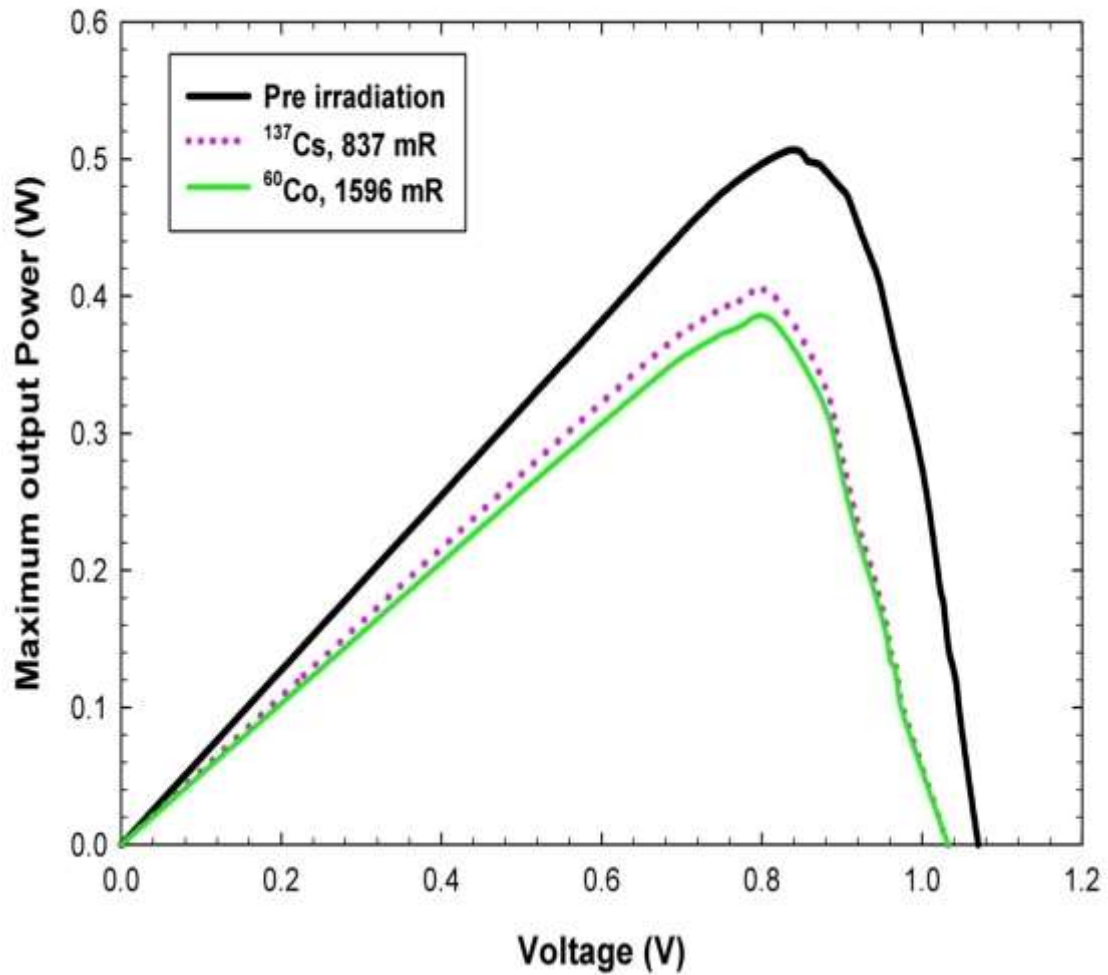


**Fig (5.8.c): The illuminated P-V characteristics of mc-Si solar cell irradiated with 1596 mR <sup>60</sup>Co gamma photons VS 837 mR <sup>137</sup>Cs gamma.**

## 5.7. Conclusions

The research involved in this work, discusses the gamma-induced defects in Silicon-based solar power systems. The experimental methods are used to investigate the impact of  $^{60}\text{Co}$  and  $^{137}\text{Cs}$  gamma ray photons on the electrical properties of Silicon-based solar power systems.

The hypothesis of this work is based on the fact that  $\gamma$  radiation damage is induced by the ionization and excitation of the atoms within the junction space charge region of a junction device such as solar cell. The presence of impurity atoms that are either added to the base material as donors, or during the manufacturing process, has indicated the possibility that some of the produced electrons might be trapped by those atoms between the valence and conduction band. Consequently, the output of the optoelectronic device exposed to  $\gamma$  radiation is also reduced. This reduction can be highly affected by the amount of gamma radiation dose which the device absorbs.

As hypothesized, the results confirmed the significant impact of  $^{60}\text{Co}$  and  $^{137}\text{Cs}$   $\gamma$ -induced displacement damage on photovoltaic parameters of mc-Si solar cells. As the  $^{60}\text{Co}$   $\gamma$ - exposure doses are increased; 532mR, 1064 and 1596 mR, a deterioration of the electric properties of mc-Si solar cell was observed.

The  $V_{mp}$  values after irradiation were decreased by 0.4%, 2.9%, 9% respectively while  $I_{mp}$  values after irradiation were deteriorated by 9.7%, 12% and 17.5%, respectively. Consequently, the maximum output power values were deteriorated by approximately 10%, 14.5% and 24.9%, respectively. The  $V_{oc}$  and  $I_{sc}$  values were deteriorated by approximately 1.5%, 2.2% and 3% for

$V_{oc}$ , and 3%, 6% and 11.9% for  $I_{sc}$ , respectively. On the other hand, the FF values deteriorated by 5.9%, 7.1% and 12.2% respectively. while the  $\eta$  values deteriorated by 9%, 13.4% and 24% respectively.

Similarly As the  $^{137}\text{Cs}$   $\gamma$ - exposure doses are increased; 280mR, 560mR and 837 mR, a deterioration of the electric properties of mc-Si solar cell was observed. The  $V_{mp}$  values were decreased by 0.4%, 2.9%, 9% respectively, while  $I_{mp}$  values were deteriorated by 7.9%, 10.1% and 13.3%, respectively. Consequently, the maximum output power values were deteriorated by approximately 8.3%, 12.8% and 21.1%, respectively. The  $V_{oc}$  and  $I_{sc}$  values were deteriorated by approximately 0.9%, 1.6% and 2% for  $V_{oc}$ , and 2%, 5% and 10.9% for  $I_{sc}$ , respectively. Moreover the FF values deteriorated by 5.5%, 6.8% and 9.7%. while the  $\eta$  values deteriorated by 7.1%, 11.7% and 20.2% respectively.

When comparing the I-V reduction caused by  $^{60}\text{Co}$   $\gamma$ -ray photons to that caused by  $^{137}\text{Cs}$   $\gamma$ -ray photons at the same acquisition time, it was found that the  $V_{mp}$  reduction caused by  $^{60}\text{Co}$   $\gamma$ -ray photons exceeds that of  $^{137}\text{Cs}$   $\gamma$ -ray photons by 0.04% for 1hr exposure, 0.0001% for 2hrs exposure.

While for 3hrs exposure the  $V_{mp}$  reduction by  $^{60}\text{Co}$   $\gamma$ -ray photons exceeds that of  $^{137}\text{Cs}$   $\gamma$ -ray photons by 0.001%.

Similarly when comparing the  $I_{mp}$  reduction caused by  $^{60}\text{Co}$   $\gamma$ -ray photons to that caused by  $^{137}\text{Cs}$   $\gamma$ -ray photons at the same acquisition time (1,2,3 hrs), it was found that the  $I_{mp}$  reduction caused by  $^{60}\text{Co}$   $\gamma$ -ray photons exceeds that of

$^{137}\text{Co}$   $\gamma$ -ray photons by 1.96% , 2% , 4.9% respectively. Similarly the P-V reduction caused by  $^{60}\text{Co}$   $\gamma$ -ray photons exceeds that of  $^{137}\text{Co}$   $\gamma$ -ray photons by 4.9% at the same acquisition time (3 hrs).

On the other hand when comparing the P-V reduction caused by  $^{60}\text{Co}$   $\gamma$ -ray photons with that caused by  $^{137}\text{Cs}$   $\gamma$ -ray photons at the same acquisition time (1,2,3 hrs) for both sources, it was found that the  $P_{mp}$  reduction caused by  $^{60}\text{Co}$   $\gamma$ -ray photons exceeds that of  $^{137}\text{Cs}$   $\gamma$ -ray photons by 2% 1.9% 4.7% respectively . This may attribute to the fact that the average energy of  $^{60}\text{Co}$  (1.25 Mev) is higher than the energy of  $^{137}\text{Cs}$  (0.662 Mev).

In terms of degradation of photovoltaic parameters for the mc-Si solar cell under  $^{60}\text{Co}$  and  $^{137}\text{Cs}$   $\gamma$  irradiation, the results are in good agreement with the available literature.

## **5.8. Recommendations**

The use of solar cells to provide electric power for communication and experiment purposes is almost universal. These devices, which convert solar energy directly to electric power with an initial efficiency of about 10 percent, suffer radiation damage in space [56]. Among other types of radiation, the damage is mainly due to bombardment by photons. Thus, it is important to develop types of solar cells, with suitable transparent radiation shields, which minimize this damage. As recommendations, transparent materials are important to cover solar cells for shielding in a radiation environment. These cover materials must not discolor in a radiation environment.

Among different shielding materials, Synthetic fused quartz is the most frequently used material because of its radiation resistance [57]. Fused-quartz covers are somewhat expensive to produce because they have to be cut to size and ground and polished to the desired thickness (usually between 0.076 and 0.76 mm) and surface quality. Annealed sapphire, which is even more radiation resistant than fused quartz, has also been used as solar -cell cover material; however, sapphire is a very expensive material. The other frequently used cover material is corning glass (Micro-Sheet). This glass has a thermal coefficient of linear expansion that more closely matches the silicon solar-cell material than does fused quartz.

## References

- [1] Cuce E, Cuce PM and Bali T, An experimental analysis of illumination intensity and temperature dependency of photovoltaic cell parameters. *App. Energy*, 111(2013)374–382.
- [2] Singh P and Ravindra NM, Temperature dependence of solar cell performance an analysis, *Sol. Energy Mater. Sol. Cells*, 101(2012) 36–45.
- [3] O. Tuzun, S. Altındal, S. Oktik, Effects of illumination and  $^{60}\text{Co}$   $\gamma$ -ray irradiation on the electrical characteristics of porous silicon solar cells, *Renew. Energy*, 3 (2008) 286.
- [4] Junga FA and Enslow GM, Radiation Effects in Silicon Solar Cells. *IRE transactions on nuclear science*. 6(1959) 49-53.
- [5] G. Holmes-Siedle and L. Adams, *Handbook of Radiation Effects*, Oxford University Press., Oxford, UK, 2nd edition, (2002).
- [6] J. L. Barth, C. S. Dyer, and E. G. Stassinopoulos, “Space, atmospheric, and terrestrial radiation environments,” *IEEE Transactions on Nuclear Science*, 50(2003)466–482.
- [7] V. S. Vavilov and N. A. Ukhin, *Radiation Effects in Semiconductors and Semiconductor Devices*, Consultants Bureau, New York, NY, USA, (1977).
- [8] R. Radosavljević and A. Vasić, “Effects of radiation on solar cells as photovoltaic generators,” *Nuclear Technology & Radiation Protection*, 27(2012)28–32.
- [9] D. Nikolić, A. Vasić, I. Fetahović, K. Stanković, and P. Osmokrović, “Photodiode behavior in radiation environment,” *Scientific Publications of the State University of Novi Pazar A*, 3(2011)27–34.

- [10] R. J. Walters, S. R. Messenger, H. L. Cotal, G. P. Summers and E. A. Burke, *Solid-State Electron, Int. J. Electrochem. Sci*, 8 (2013) 7841.
- [11] L. Musilek, P. Fowles, Directional dependence of solar cells used as monitors of high  $\gamma$ -ray dose rates, *Int. J. Appl. Rad. Isotopes*, 33 (1982) 1473.
- [12] S. Asdul-Majid, Use of a solar panel as a directionally sensitive large-area radiation monitor for direct and scattered x-rays and gamma-rays, *International Journal of Radiation Applications and Instrumentation Part A Applied Radiation and Isotopes* , 38 (1987) 1057.
- [13] G. P. Summers, et al, Damage Correlations in Semiconductors Exposed to Gamma, Electron and proton Radiation, *IEEE Trans. Nucl. Sci*, 40 (1993) 1372-1379.
- [14] T. P Ma, P. V Dressendorfer, *Ionizing radiation effect in MOS devices and circuits*, Wiley, New York, (1989).
- [15] M. Yamaguchi, Radiation-resistant solar cells for space use, *Solar Energy Materials and Solar Cells*, 68 (2001) 31-53.
- [16] D. J. Curtin, R.L. Statler, Review of radiation damage to silicon solar cells, *IEEE Trans. Aerospace Electron Systems*, 11 (1975) 499 - 513.
- [17] J. Dubow, Hydrogen and methane synthesis through radiation catalysis, US DOE Report, DOEER-4258-T-1, (1980) 45.
- [18] H.Y. Tada, J.R. Carter, B.E. Anspaugh, R.G. Downing, *Solar Cell Radiation Handbook*, 3rd Edition, National Aeronautics and Space Administration, JPL Publication, Pasadena, California, (1982) 162.

- [19] R. D. Evans, *The Atomic Nucleus*, McGraw-Hill, New York, ch. 25 (1955).
- [20] K. Ali, S. A. Khan, M. Z. MatJafri, Low cost anisotropic etching of monocrystalline Si (100): Optimization using response surface methodology, *Superlattices and Microstructures*, 52 (2012) 782–792.
- [21] G. Xue, Y. Guo, T. Yu, J. Guan, X. Yu, J. Zhang, J. Liu, Z. Zou, Degradation Mechanisms Investigation for Long-term Thermal Stability of Dye-Sensitized Solar Cells, *Int. J. Electrochem. Sci.*, 7 (2012) 1496 – 1511.
- [22] J. R. Srour, C. J. Marshal and Paul W. Marshall, Review of displacement damage effects in silicon devices, *IEEE transactions on nuclear science*, 50 (2003) 653-670.
- [23] Junga FA and Enslow GM, Radiation Effects in Silicon Solar Cells. *IRE transactions on nuclear science*. 6(1959) 49-53.
- [24] J. J. Loferski and P. Rappaport, Radiation damage in Ge and Si detected by carrier lifetime changes: damage thresholds, *Phys. Rev*, 3 (1958) 432.
- [25] Space radiation effects on electronic components in low-earth orbit – nasa practice no. pd-ed-1258 page 1 of 7 april 1996
- [26] Globus, Al (10 July 2002). "Appendix E: Mass Shielding". *Space Settlements: A Design Study*. NASA. Retrieved 24 February 2013.
- [27] Atkinson, Nancy (24 January 2005). "Magnetic shielding for spacecraft". *The Space Review*. Retrieved 24 February 2013.
- [28] J. Lee, D. H. Kah, H. J. Kim, H. B. Park and J. H. So, Radiation Hardness Study for Silicon Strip Sensors Using the 35-MeV Proton Beam from the MC-50 Cyclotron at the Korea Institute of Radiological and Medical Sciences. *J Journal of the Korean Physical Society*, 48(2006) 850-854.



[29] R.Gunnink J.E.Evans and A.L. Prindle “A Reevaluation of the Gamma Ray Energies and Absolute Branching Intensities of  $^{237}\text{U}$   $^{238,239,240,241}\text{Pu}$  and  $^{241}\text{Am}$  “Lawrance Livermore Laboratory report UCRL-52139 (1976).

[30] H. J. Hyun, et al, Radiation Damage Study of AC-Coupled Silicon Strip Sensors with a Proton Beam, Journal of the Korean Physical Society, 50 (2007) 1548-1551.

[31] J. Bahr, Microwave Nondestructive Testing Methods, New York: Gordon and Breach, (1982).

[32] H. Burger, Nondestructive testing. U. S. Atomic Energy Commission, (1967).

[33] J. S. Charlton and E. F. Wellman, Quality measurement in industrial process plants - the role of radioisotopes, Applied Radiation and Isotopes, 41(1990)1067–1077.

[34] A. Van Ginneken, Non-ionizing Energy deposition in Silicon for Radiation Damage Studies, Fermi lab National Accelerator Laboratory FN-522, (1989).

[35] Junhyun Kwon, Arthur T. Motta, Gamma displacement cross-sections in various materials. Annals of Nuclear Energy ,27 (2000) 1627-1642.

[36] Robert J. Walters et al, Modeling of Radiation Induced Defects in Space Solar Cells, Proceedings of SPIE, The International Society for Optical Engineering, February (2011).

[37] H.M. Diab, A. Ibrahim, And R. Elmallawany, Silicon solar cells as a gamma ray dosimeter, Measurement, 46(2013) 3635-3639.

[38] Davud Mostafa Tobnaghi, Ali Rahnamaei, Mina Vajdi, Experimental Study of Gamma Radiation Effects on the Electrical Characteristics of Silicon Solar Cells, Int. J. Electrochem. Sci., 9 (2014) 2824 – 2831.

- [39] M. Alurraldea, M.J.L. Tamasib and C.J. Brunob, Experimental and theoretical radiation damage studies on crystalline silicon solar cells, *Solar Energy Materials & Solar Cells* , 82(4)(2004), 531-542.
- [40] Heydar Mahdavi and Rahim Madatov, Effect of Irradiation on Electrical Conduction and Crystallization in Ge<sub>1-x</sub>Si<sub>x</sub> Films, *International Journal of Electrochemical Science*, 9 (2014) 1179-1186.
- [41] A. Vasić, M. Vujisić, B. Lončar, And P. Osmokrović, Temperature and radiation hardness of polycarbonate capacitors, *Journal of Optoelectronics and Advanced Materials*, 9 (2007) 2863-2866.
- [42] Oen and Holmes, Cross Sections for Atomic Displacement in Solid by Gamma Rays , *AIP Journal of Applied Physics*, 30(1959) 1289.
- [43] M. Zdravkovic, A. Vasić, R. Radosavljević, M. Vujisić, and P. Osmokrovic, Influence of radiation on the properties of solar cells, *Nuclear Technology & Radiation Protection*, 26 (2011) 158–163.
- [44] Statler, RL, Radiation damage and annealing of lithium-doped silicon solar cells, Naval Research Lab., Washington, DC, United States, (1971).
- [45] Seitz F and Koehler JS, Displacement of atoms during irradiation in solid state physics. Seitz F and Turnbull D, editors., Academic Press, Inc., New York, N. Y., vol. 2, (1956).
- [46] Hovel J, *Semiconductors and Semimetals*, Academic Press, New York. Messenger GC and Ash MS, *The effects of radiation on electronic systems*, Van NostrandReinhold, New York, (1975).
- [47] Alexander DR, Transient ionizing radiation effects in devices and circuits. *IEEE Transaction on Nuclear Sciences*, 50(2003)565-582.

[48] Horiushi N, Nozaki T, and Chiba A, Improvement in electrical performance of radiationdamaged silicon solar cells by annealing, NIM A, 443(2000)186-193.

[49] Yukahe TC, Studying photovoltaic parameters of the aging silicon solar cells by thermal annealing. International Journal of Advanced and Applied Sciences, 1(6) (2014)1-6.

[50] Guseynov NA, Olikh YaM and Askerov ShG, Ultrasonic treatment restores the photovoltaic parameters of silicon solar cells degraded under the action of  $^{60}\text{Co}$  gamma radiation, Technical Physics Letters, 33 (2007) 18-21.

[51] [www.leybold.com](http://www.leybold.com).

[52] Irwan YM, Leow WZ , Irwanto M, Fareq.M , Amelia AR, Gomesh N and Safwati I, Indoor test performance of pv panel through water cooling method, Energy Procedia, 79(2015) 604-611.

[53] Khan F, Singh SN and Husain M, Effect of illumination intensity on cell parameters of a silicon solar cel, Solar Energy Materials & Solar Cells, 94(2010)1473–1476.

[54] Van Oventraeten R J and Mertens RP, Physics technology and use of phorovollaics, Bristol: Adam Hilger, ch 2(1986).

[55] Sathyanarayana, et al, A study on the variation of C-Si solar cell parameters under 8 MeV electron irradiation, Solar Energy Materials and Solar Cells, 120 (2014) 191-196.

[56] Ramond C. Waddel, Radiation Damage Shielding Of Solar Cells on A Synchronous Spacecraft, NASA-Goddard Space Flight Center, Spacecraft Technology Division, (1968).

[57] Gilbert A. Haynes, Effect of Radiation on Cerium-Doped Solar Cell Cover Glass, Langley Research Center, Hampton, Va. 23365, (1970).